

Mechanical System Design Fundamentals

Andrew Ning
Brigham Young University
ME 372
Version: April 16, 2019
Copyright © 2019 Andrew Ning

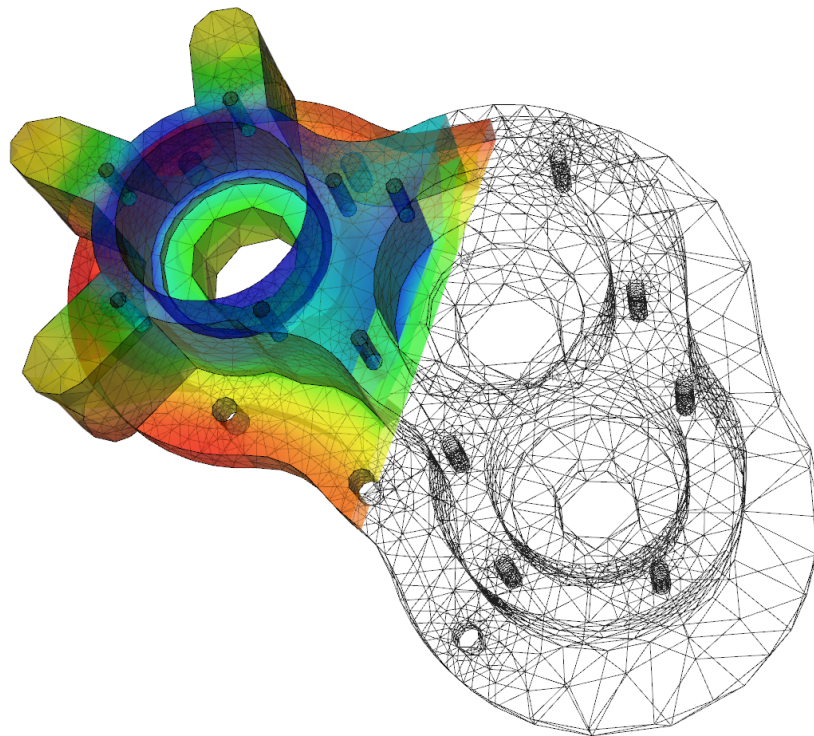


Figure from User A1, [Wikimedia Commons](#), CC BY-SA 3.0.

Contents

1	Stress and Strain	7
1.1	Stress	7
1.2	Strain	10
1.3	Plane Stress and Plane Strain	12
1.4	Materials	12
1.4.1	Linear Stress-Strain Relationships	13
1.4.2	Material Properties	15
1.5	Plane-Stress Transformation	18
1.5.1	Principal Stresses	19
1.5.2	Mohr's Circle	21
2	Combined Loads	24
2.1	Axial Stress	24
2.2	Bending Stress	25
2.2.1	Neutral Axis	28
2.2.2	Moments of Inertia	29
2.2.3	Bidirectional Bending	31
2.3	Direct Shear	32
2.4	Shear from Bending	33
2.5	Torsion	35
2.6	Combined Loads	38
2.7	Stress Concentrations	45
3	Cylinders	47
3.1	Pressure Vessels	47
3.2	Thin Pressure Vessel	50
3.3	Press/Shrink Fits	51

4	Deflection	55
4.1	Strain Energy	55
4.2	Castigliano's Theorems	58
4.2.1	Existing Loads	59
4.2.2	Dummy Loads	61
4.2.3	Statically Indeterminate Structures	63
5	Static Failure	65
5.1	Maximum Shear Stress Theory	65
5.2	Distortion Energy Theory	67
5.2.1	Yield Strength in Shear	70
5.3	Coulomb-Mohr Theory for Ductile Materials	70
6	Unsymmetric Bending	73
6.1	Moments of Inertia	73
6.2	Unsymmetric Bending of Straight Beams	75
7	Buckling	78
7.1	Euler Column Buckling	78
7.2	Johnson Buckling	83
8	Reliability	85
8.1	Brief Statistics Review	85
8.1.1	Random Variables	85
8.1.2	Expectation and Variance	86
8.1.3	Common Probability Distribution	87
8.1.4	Forward Propagation	88
8.2	Reliability	89
9	Fatigue	93
9.1	Process	93
9.2	Case 1: Fully Reversed Simple Loading	94
9.3	Case 2: Fluctuating Simple Loading	95
9.4	Case 3: Combined Simple Loading	96
10	Fatigue 2	99
10.1	Introduction	99
10.2	Endurance Limit	101
10.2.1	Surface Finish	101
10.2.2	Size	102
10.3	Fully Reversed Load	102

10.4 Simple Fluctuating Load	102
10.5 Combined Fluctuating Loads	102
10.6 Complex Loads	102
A Cylinder Theory Derivation	103
B Unsymmetric Bending Derivation	108
C Standard Normal Table	110

Acknowledgments

A few of the figures and examples come directly from Dr. Jon Blotter, used with permission. I'm also indebted to Jon for teaching this material to me when I was an undergraduate.

Preface

This book is developed for the purpose of helping students in BYU's ME 372: Mechanical System Design Fundamentals class. It is being created just-in-time for the class so don't expect a polished product. Words in *italics* indicate important terminology.

Segments that are indented like this paragraph are meant to denote tangents or advanced topics that are not required, but are provided for the interested reader. Advanced topics or derivations that are longer are placed in the Appendix.

Currently, the text primarily focuses on explaining core concepts and equations and is light on examples. The intent is that reading the textbook will provide necessary background material freeing up time to discuss more examples during class.

Chapter 1

Stress and Strain

Stress and strain are fundamental concepts in structural analysis, especially with regards to predicting structural failure. Material properties provide the connection between stress and strain.

1.1 Stress

Stress is defined as a force per unit area. The SI units of stress are N/m^2 or Pa (pascals). In Imperial units stress is often given in pounds per square inch (psi) or kilopounds per square inch (kpsi or ksi). Figure 1.1 shows an example of one-dimensional stress in a bar given by the following formula:

$$\sigma = \frac{F}{A} \quad (1.1)$$

where σ is the stress.

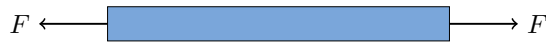


Figure 1.1: One-dimensional stress in a bar.

More generally, stress is defined by both by the direction of the force and the orientation of the face upon which the force acts. This type of quantity is not a vector but is called a tensor. For our purposes we can think of a tensor as a matrix, although a tensor is actually more general than that. At a given point, stress is a tensor with nine components as shown in Fig. 1.2

and represented mathematically as:

$$\boldsymbol{\sigma} = \begin{bmatrix} \sigma_{xx} & \tau_{xy} & \tau_{xz} \\ \tau_{yx} & \sigma_{yy} & \tau_{yz} \\ \tau_{zx} & \tau_{zy} & \sigma_{zz} \end{bmatrix} \quad (1.2)$$

We only needed to draw the stresses on three faces, because from static equilibrium we can show that the stresses are equal and opposite on the opposite faces.

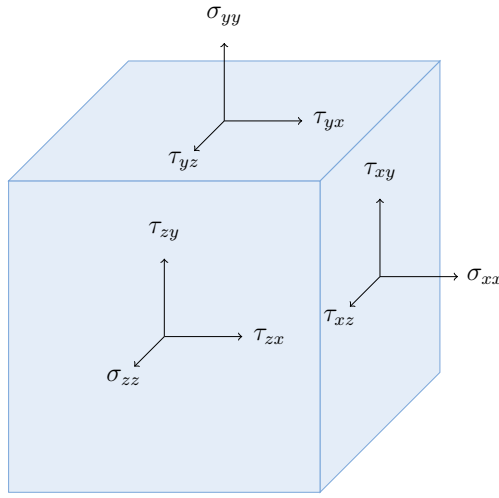


Figure 1.2: The stress at any point in some material has nine components but only six are independent (a symmetric second order tensor).

The first index indicates the orientation of the face (e.g., x indicates a face whose normal points in the positive x direction), and the second index indicates the direction of the stress. Normal stress is denoted by σ and acts normal to a face. Normal stress involves tension or compression. Usually, for convenience, the second index on normal stresses is dropped (i.e., σ_x , σ_y , σ_z). Shear stress is denoted by τ and acts in the plane of the face. The stress τ_{xy} , for example, indicates a shear stress on the x face in the y direction. Shear stresses rotate or shear the structure. Figure 1.3 shows examples of pure tension, compression, and shear (rotation, while applicable to fluid dynamics, is generally irrelevant for structures).

Although we have shown nine components in the stress tensor, only six of them are independent. From conservation of angular momentum we can show that $\tau_{xz} = \tau_{zx}$, $\tau_{xy} = \tau_{yx}$, and $\tau_{yz} = \tau_{zy}$ (and thus the ordering of

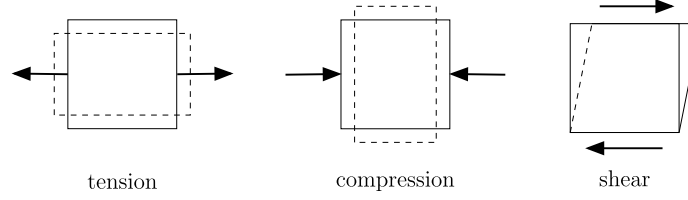


Figure 1.3: Examples of tension, compression, and shear

the indices is not really important). The positive sign conventions (for a 2D section) are shown in Fig. 1.4.

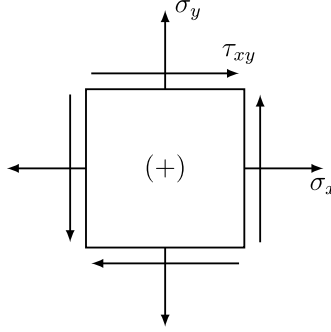


Figure 1.4: Positive sign convention for stresses.

Generally when we say stress what we mean is *nominal stress* (also known as engineering stress). Nominal stress is the stress computed using the undeformed configurations (see top figure in Fig. 1.5). However, there is an alternative: *true stress* in which both the force and area are measured in the deformed configuration (see bottom figure in Fig. 1.5). For most engineering problems the difference is irrelevant, as significant changes in area generally only occur close to failure. The reduction in area is called *necking*.

Our definition of the stress tensor was given for a particular coordinate system, but stress can be defined for any coordinate system. The force per unit area on a general surface with normal \mathbf{n} (called the traction vector, \mathbf{t}) is given by:

$$\mathbf{t} = \boldsymbol{\sigma} \cdot \hat{\mathbf{n}} \quad (1.3)$$

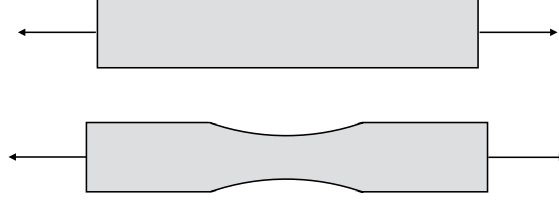


Figure 1.5: Nominal stress is based on cross-sectional areas on the undeformed configuration (top). True stress is based on cross-sectional areas using the deformed configuration (bottom).

1.2 Strain

Strain is a measure of deformation. One-dimensional axial strain is given by:

$$\epsilon = \frac{\Delta l}{l_0} \quad (1.4)$$

using the definitions shown in Fig. 1.6.

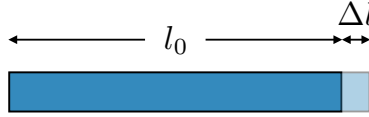


Figure 1.6: One-dimensional strain is the change in length relative to the original length.

In general, both ends of the bar could displace. Then the strain is defined as shown in the equation below using the definitions in Fig. 1.7. We see that this expression looks a lot like a numerical derivative, and indeed as we go to the limit of $dx \rightarrow 0$ the strain is defined as $\epsilon_x = \partial u / \partial x$. Like stress, strain is defined at a given point and can vary throughout the object.

$$\epsilon = \frac{u_1 - u_0}{x_1 - x_0} \rightarrow \frac{\partial u}{\partial x} \quad (1.5)$$

Also like stress, there are three normal strains and three shear strains. Displacements in the x , y , and z direction will be referred to as u , v , and w



Figure 1.7: A more general representation of one-dimensional strain where both ends of the bar displace.

respectively. The normal strain are given by:

$$\begin{aligned}\epsilon_x &= \frac{\partial u}{\partial x} \\ \epsilon_y &= \frac{\partial v}{\partial y} \\ \epsilon_z &= \frac{\partial w}{\partial z}\end{aligned}\tag{1.6}$$

The shear strain components are defined by changes in angles. Referring to Fig. 1.8, the in-plane component of shear strain is given by:

$$\gamma_{xy} = \theta_1 + \theta_2\tag{1.7}$$

For small angles (which becomes exact in the limit):

$$\theta_1 \approx \tan \theta_1 = \frac{\Delta v}{\Delta x} \rightarrow \frac{\partial v}{\partial x}\tag{1.8}$$

Similarly,

$$\theta_2 \approx \tan \theta_2 = \frac{\Delta u}{\Delta x} \rightarrow \frac{\partial u}{\partial y}\tag{1.9}$$

The three shear strain components are thus given as:

$$\begin{aligned}\gamma_{xy} &= \gamma_{yx} = \frac{\partial v}{\partial x} + \frac{\partial u}{\partial y} \\ \gamma_{yz} &= \gamma_{zy} = \frac{\partial w}{\partial y} + \frac{\partial v}{\partial z} \\ \gamma_{xz} &= \gamma_{zx} = \frac{\partial u}{\partial z} + \frac{\partial w}{\partial x}\end{aligned}\tag{1.10}$$

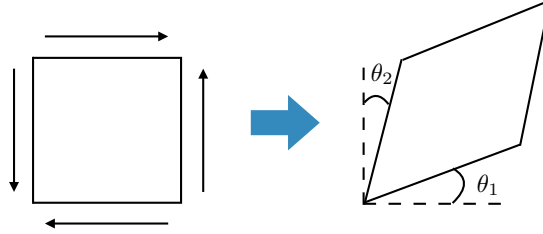


Figure 1.8: Illustration of shear strain.

1.3 Plane Stress and Plane Strain

In this book we will often analyze *plane stress* scenarios. These occur when all of the stresses are in a plane, or in other words, when all the stresses on one of the surfaces in Fig. 1.2 are zero (e.g., $\sigma_{zz} = 0$, $\tau_{xz} = 0$, $\tau_{yz} = 0$). Figure 1.4 is a representation of plane stress. Note that there are only three nonzero components of stress in that case. Plane stress occurs when all of the loads are in a plane and (generally) when the structure is also thin in the out-of-plane dimension. Some examples include a wrench, the skin of an aircraft wing, a soda can, a planar truss, etc. Real structures always have three-dimensional stress states, so plane stress is an idealization, but a useful idealization for many engineering problems.

Plane strain occurs when all of the nonzero strains are in a plane. This scenario occurs when a body cannot expand or contract in a particular direction (e.g., $\epsilon_{zz} = \gamma_{xz} = \gamma_{yz} = 0$). Some examples include a pressure vessel constrained on both ends, or for a very thick structure like a dam. Usually, plane stress and plane strain don't exist simultaneously. In this text we will often see plane stress scenarios; plane strain scenarios will be less common.

1.4 Materials

Material properties provide the link between stresses and strains. A material is said to be *homogeneous* if its properties are the same throughout. A material is said to be *isotropic* if its properties are the same in every direction. In this text we will focus on materials that are both homogeneous and isotropic, but in this section we will provide some broader context for the behavior of more general materials.

1.4.1 Linear Stress-Strain Relationships

For a general material in the elastic region the six components of stress and the six components of strain can be related as:

$$\begin{bmatrix} \epsilon_x \\ \epsilon_y \\ \epsilon_z \\ \gamma_{xy} \\ \gamma_{xz} \\ \gamma_{yz} \end{bmatrix} = \begin{bmatrix} S_{11} & S_{12} & S_{13} & S_{14} & S_{15} & S_{16} \\ S_{21} & S_{22} & S_{23} & S_{24} & S_{25} & S_{26} \\ S_{31} & S_{32} & S_{33} & S_{34} & S_{35} & S_{36} \\ S_{41} & S_{42} & S_{43} & S_{44} & S_{45} & S_{46} \\ S_{51} & S_{52} & S_{53} & S_{54} & S_{55} & S_{56} \\ S_{61} & S_{62} & S_{63} & S_{64} & S_{65} & S_{66} \end{bmatrix} \begin{bmatrix} \sigma_x \\ \sigma_y \\ \sigma_z \\ \tau_{xy} \\ \tau_{xz} \\ \tau_{yz} \end{bmatrix} \quad (1.11)$$

or

$$\boldsymbol{\epsilon} = \mathbf{S}\boldsymbol{\sigma} \quad (1.12)$$

where \mathbf{S} is called the compliance matrix and can be shown to be symmetric. Thus, in this general case there are 21 independent constants needed to define the material properties. These are called the *constitutive relationships* and can also be written as the inverse mapping:

$$\boldsymbol{\sigma} = \mathbf{K}\boldsymbol{\epsilon} \quad (1.13)$$

where $\mathbf{K} = \mathbf{S}^{-1}$ is the stiffness matrix. The stiffness matrix is also symmetric (from linear algebra we know that the inverse of a symmetric matrix is also symmetric).

Usually, a material has certain symmetries. *Orthotropic* materials have three orthogonal planes of symmetry and in that case the compliance matrix can be reduced to:

$$\begin{bmatrix} \epsilon_x \\ \epsilon_y \\ \epsilon_z \\ \gamma_{xy} \\ \gamma_{xz} \\ \gamma_{yz} \end{bmatrix} = \begin{bmatrix} S_{11} & S_{12} & S_{13} & 0 & 0 & 0 \\ S_{21} & S_{22} & S_{23} & 0 & 0 & 0 \\ S_{31} & S_{32} & S_{33} & 0 & 0 & 0 \\ 0 & 0 & 0 & S_{44} & 0 & 0 \\ 0 & 0 & 0 & 0 & S_{55} & 0 \\ 0 & 0 & 0 & 0 & 0 & S_{66} \end{bmatrix} \begin{bmatrix} \sigma_x \\ \sigma_y \\ \sigma_z \\ \tau_{xy} \\ \tau_{xz} \\ \tau_{yz} \end{bmatrix} \quad (1.14)$$

There are now only 12 unknowns, but they actually depend on only 9 independent variables: E_{11} , E_{22} , E_{33} , G_{12} , G_{13} , G_{23} , ν_{12} , ν_{13} , ν_{23} , where E_{ii} is the Young's modulus along axis i , G_{ij} is the shear modulus in direction j on the plane whose normal is in direction i , and ν_{ij} is the Poisson's ratio that corresponds to a contraction in direction j when an extension is applied in direction i . Many composites and woods are orthotropic materials.

A special case of orthotropy is isotropy, in which the elastic properties are the same in every direction. The compliance matrix looks similar in form, but the 12 unknowns reduce to 2 independent constants: E the modulus of elasticity, and ν Poisson's ratio. The full matrix looks like the following:

$$\begin{bmatrix} \epsilon_x \\ \epsilon_y \\ \epsilon_z \\ \gamma_{xy} \\ \gamma_{xz} \\ \gamma_{yz} \end{bmatrix} = \frac{1}{E} \begin{bmatrix} 1 & -\nu & -\nu & 0 & 0 & 0 \\ -\nu & 1 & -\nu & 0 & 0 & 0 \\ -\nu & -\nu & 1 & 0 & 0 & 0 \\ 0 & 0 & 0 & 2(1+\nu) & 0 & 0 \\ 0 & 0 & 0 & 0 & 2(1+\nu) & 0 \\ 0 & 0 & 0 & 0 & 0 & 2(1+\nu) \end{bmatrix} \begin{bmatrix} \sigma_x \\ \sigma_y \\ \sigma_z \\ \tau_{xy} \\ \tau_{xz} \\ \tau_{yz} \end{bmatrix} \quad (1.15)$$

The inverse relationship (using the stiffness matrix) looks like:

$$\begin{bmatrix} \sigma_x \\ \sigma_y \\ \sigma_z \\ \tau_{xy} \\ \tau_{xz} \\ \tau_{yz} \end{bmatrix} = \frac{E}{(1+\nu)(1-2\nu)} \begin{bmatrix} 1-\nu & \nu & \nu & 0 & 0 & 0 \\ \nu & 1-\nu & \nu & 0 & 0 & 0 \\ \nu & \nu & 1-\nu & 0 & 0 & 0 \\ 0 & 0 & 0 & \frac{1-2\nu}{2} & 0 & 0 \\ 0 & 0 & 0 & 0 & \frac{1-2\nu}{2} & 0 \\ 0 & 0 & 0 & 0 & 0 & \frac{1-2\nu}{2} \end{bmatrix} \begin{bmatrix} \epsilon_x \\ \epsilon_y \\ \epsilon_z \\ \gamma_{xy} \\ \gamma_{xz} \\ \gamma_{yz} \end{bmatrix} \quad (1.16)$$

Most metals are (nearly) isotropic, and everything in this text will assume isotropy.

Although you may not be familiar with these equations in matrix form, the relationships should be familiar from an introductory mechanics of materials course. For example, the strain in the x-direction is (using the first row of the compliance matrix):

$$\epsilon_x = \frac{1}{E} [\sigma_x - \nu(\sigma_y + \sigma_z)] \quad (1.17)$$

The one-dimensional version should be familiar (with subscripts dropped) $\sigma = E\epsilon$, and likely the two-dimensional version as well.

The shear stresses take the form (using the fourth row of the stiffness matrix):

$$\tau_{xy} = \frac{E}{2(1+\nu)} \gamma_{xy} \quad (1.18)$$

Notice that unlike normal strain, the shear strain/stress relationship does not include any off-diagonal components. For convenience, the above grouping of constants is called the shear modulus of elasticity and is given the symbol G :

$$G = \frac{E}{2(1+\nu)} \quad (1.19)$$

This is not a new constant, just a convenient definition that allows us to express the shear stress/strain relationships as:

$$\tau_{xy} = G\gamma_{xy} \quad (1.20)$$

Note from the stress transformation equations that just because the normal strain in a given direction is zero, the normal stress in that same direction might not be zero (for example in a constrained pressure vessel). The reverse is also true.

1.4.2 Material Properties

Let us examine these material properties in more detail. The *modulus of elasticity*, or *Young's modulus* E is a measure of material stiffness. For one-dimensional isotropic elastic loading we found that we can relate stress and strain as:

$$\sigma = E\epsilon \quad (1.21)$$

The constant E is the slope in the linear region of the stress-strain curve in Fig. 1.9, from the origin to point p . Note that the figure shows stress and strain rather than force and deflection. The reason for this is that plotting force and deflection would require a new curve for different sizes of bars, but stress and strain collapse to one curve allowing us to isolate the effect of the material. Point p is called the proportional limit, beyond this point the material behavior is no longer linear.

The point e is more subtle, and less important to our discussion, but it is called the elastic limit. Beyond e the behavior is no longer *elastic*, which means that the deformation is *plastic* (i.e., permanent). From p to e the behavior is nonlinear, but still elastic. Points p to e are generally very close, or identical, so it's usually not a major distinction.

The next important point in the figure is the yield point (y), and the corresponding stress is called the yield stress. This point is often used in mechanical design because beyond the yield stress, the strain increases rapidly with small changes in stress. For this reason the yield stress is often used as a measure of failure. There is not a universally agreed upon definition of yield stress, but often it is specified by drawing a line parallel to the linear region but offset by some amount (typically 0.2% of the original length of the member, or $\epsilon = 0.002$).

Ultimate strength (u) corresponds to the absolute maximum amount of stress the material can take, and fracture strength (f) where the structure has completely fractured. Often ultimate and fracture strength occur near

each other or at the same location. Ultimate stress is sometimes a quantity of interest, but for mechanical design we are usually more concerned with staying below the yield stress.

Previously, we discussed the difference between nominal and true stress (see Fig. 1.5). If true stress were plotted the strain would actually go up between u and f as indicated by the dashed line at the upper right of the curve. However, as discussed previously, we generally just refer to nominal stress/strain, which is the solid line.

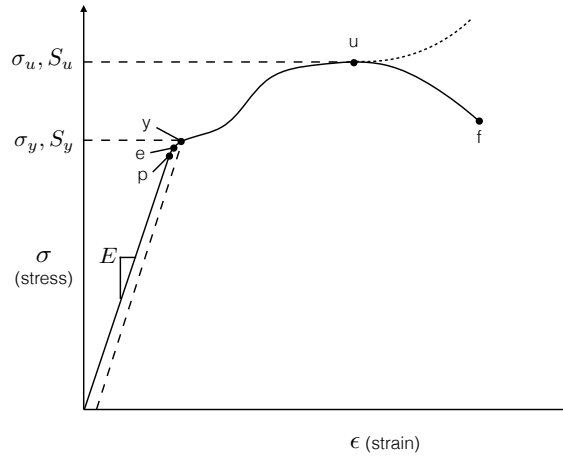


Figure 1.9: A typical stress strain curve for ductile materials.

Figure 1.9 is for *ductile* materials. Ductile materials can stretch and bend. In contrast, brittle materials will crack or break as opposed to stretching or bending. Some common examples are concrete, ceramics, and glasses. For brittle materials, yielding, ultimate strength, and fracture generally all occur at the same place. Brittle materials are often porous, which makes them very strong in compression but under tension the cracks propagate causing fracture. We will mostly concern ourselves with ductile material in this text, but will discuss some failure theories for brittle materials.

It should be noted that for some materials the strengths differ in tension versus compression. In other words, you may have significantly different values for the ultimate strength in tension S_{ut} and the ultimate strength in compression S_{uc} . Concrete is a good example of this. For most metals, the strength in tension and compression is the same.

Material properties are not exact quantities, but rather are statistical properties derived from many load tests. Because of natural variation, safety

factors are always used in engineering design. These are often derived from statistical analyses, experiments, computations, and past history.

Poisson's ratio, ν is the change in lateral strain relative to normal strain. Imagine stretching a bar in one direction, we would expect there to be some contraction in the lateral directions (see for example the first figure in Fig. 1.3). Mathematically this relationship is expressed as:

$$\epsilon_2 = -\nu\epsilon_1 \quad (1.22)$$

Figure 1.10 compares the strength versus density of various types of materials. Because we will focus on isotropic materials in this class, we will primarily be discussing metals. Metals are widely used in mechanical design because of their high strength. Composites are replacing metals in many applications. Note how they have similar strength, but are often lighter. However, they are usually more expensive and complex to manufacture. Their behavior is generally orthotropic, as we discussed previously. Ceramics can have very high strength, but often have brittle behavior, which limits their usefulness for many applications. Woods and foams are used in light-weight applications, like radio-controlled airplanes.

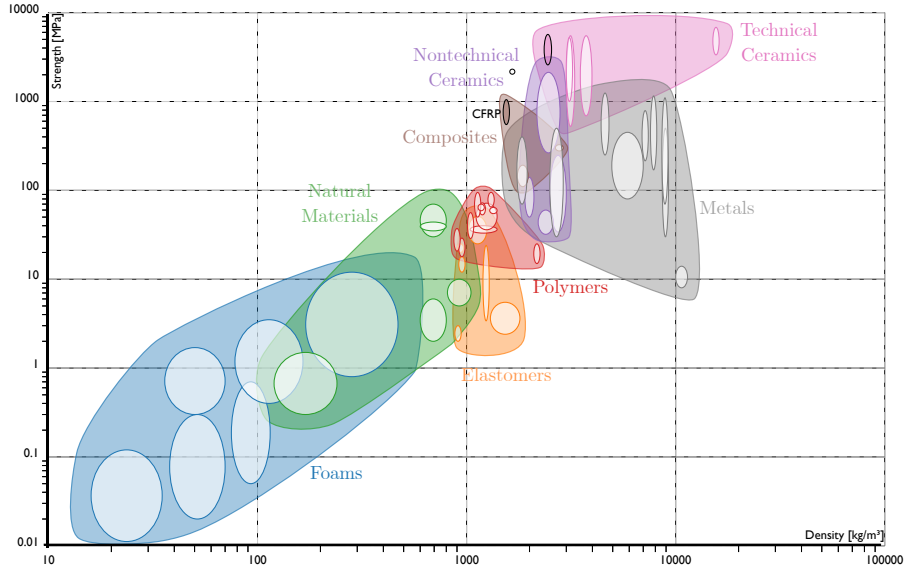


Figure 1.10: Strength versus density for various classes of materials. Figure adapted from Nicoguaro, [Wikimedia Commons](#), CC BY 4.0.

1.5 Plane-Stress Transformation

Consider the element in plane stress shown on the left hand side of Fig. 1.11. The magnitudes of the normal and shear stresses are given in the x, y coordinate system. However, this choice of coordinate system is arbitrary. Typically, we are more interested in reporting the stresses for the faces on which the stresses are maximum. Maximum stresses are of interest because they provide the critical cases for structural failure. In order to determine the faces for which stress is a maximum we first need to derive a general expression for the stresses in a rotated coordinate system.

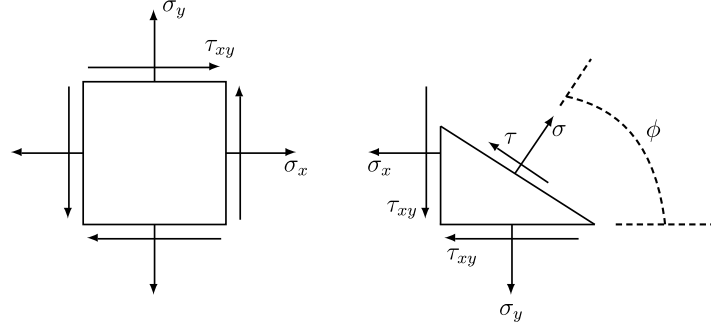


Figure 1.11: Stress can be measured in any orientation. The cut face allows us to relate stresses from the x, y orientation to some arbitrary orientation rotated by the angle ϕ .

Consider the stresses (σ, τ) on the cut face shown on the right side of Fig. 1.11. Recall that the stress vector on the cut surface is given by Eq. (1.3). For plane stress that results in the following two equations:

$$\begin{aligned} t_x &= \sigma_x n_x + \tau_{xy} n_y \\ t_y &= \tau_{xy} n_x + \sigma_y n_y \end{aligned} \quad (1.23)$$

To get the stress in the rotated coordinate system we take the dot product of the traction vector with the normal direction:

$$\sigma = \mathbf{t} \cdot \hat{\mathbf{n}} = t_x n_x + t_y n_y \quad (1.24)$$

Combining equations Eq. (1.23) and Eq. (1.24) yields

$$\sigma = \sigma_x n_x^2 + 2\tau_{xy} n_x n_y + \sigma_y n_y^2 \quad (1.25)$$

Substituting in $n_x = \cos \phi$ and $n_y = \sin \phi$ gives the transformation:

$$\sigma = \sigma_x \cos^2 \phi + \sigma_y \sin^2 \phi + 2\tau_{xy} \sin \phi \cos \phi \quad (1.26)$$

Using a few trigonometric identities ($\sin(2\phi) = 2 \sin \phi \cos \phi$, $\sin^2 \phi = (1 - \cos 2\phi)/2$, $\cos^2 \phi = (1 + \cos 2\phi)/2$) allows us to rearrange the equations in a form that will be convenient later

$$\sigma = \frac{\sigma_x + \sigma_y}{2} + \frac{\sigma_x - \sigma_y}{2} \cos 2\phi + \tau_{xy} \sin 2\phi \quad (1.27)$$

The rotated shear stress is given from the dot product of the traction vector along the direction of the cut surface \hat{s} :

$$\tau = \mathbf{t} \cdot \hat{\mathbf{s}} = -t_x \sin \phi + t_y \cos \phi \quad (1.28)$$

which after simplification and similar trigonometric identities gives a set of transformation equations:

$$\begin{aligned} \sigma &= \frac{\sigma_x + \sigma_y}{2} + \frac{\sigma_x - \sigma_y}{2} \cos 2\phi + \tau_{xy} \sin 2\phi \\ \tau &= -\left(\frac{\sigma_x - \sigma_y}{2}\right) \sin 2\phi + \tau_{xy} \cos 2\phi \end{aligned} \quad (1.29)$$

These equations allow us to compute the normal and shear stress as a function of ϕ . If we use $\phi = 0$, we should get the stresses in the x, y coordinate system, but we can now compute the stresses for any direction.

1.5.1 Principal Stresses

Now that we can compute the stresses for any orientation, we can find the orientation for which the stresses are maximized. The maximum (and minimum) stresses at a given point are called *principal stresses*.

The concept is similar to principal moments of inertia. For example, recall that the moments of inertia of a football could be computed for any coordinate system, but the principal (largest) moments of inertia occur along the symmetry axes. Ideally, a football is rotated along its largest principal axes to create a perfect spiral, otherwise it will wobble (precess) as it is thrown.

From calculus we know that extrema can be found by differentiating an expression with respect to a variable of interest and setting the result equal to zero. Differentiating the normal stress in Eq. (1.29) with respect to ϕ

and setting the result equal to zero gives the principal directions, measured relative to our x-y coordinate system (see Fig. 1.11):

$$\phi_p = \frac{1}{2} \tan^{-1} \left(\frac{2\tau_{xy}}{\sigma_x - \sigma_y} \right) \quad (1.30)$$

Note that this angle actually defines two perpendicular direction: ϕ_p , and $\phi_p + 90^\circ$. One direction contains the maximum normal stress σ_1 and the other the minimum normal stress σ_2 . However, we won't know which face contains the maximum and which contains the minimum without evaluating the stresses at both locations. Substituting this angle back into Eq. (1.29) gives the magnitude of the principal stresses

$$\boxed{\begin{aligned} \sigma_1, \sigma_2 &= \frac{\sigma_x + \sigma_y}{2} \pm \sqrt{\left(\frac{\sigma_x - \sigma_y}{2}\right)^2 + \tau_{xy}^2} \\ \tau &= 0 \end{aligned}} \quad (1.31)$$

Note that the surfaces containing the principal stresses have zero shear stress.

In a similar manner we can find the maximum shear stresses. These occur at:

$$\phi_s = \frac{1}{2} \tan^{-1} \left(-\frac{(\sigma_x - \sigma_y)}{2\tau_{xy}} \right) \quad (1.32)$$

It is straightforward to show (though not proven here) that the angles for maximum shear stress are $\pm 45^\circ$ from the surfaces containing the principal stresses. In other words, there is no need to compute ϕ_s if we have already computed ϕ_p . Substituting this angle back in to our stress expression we find the maximum shear stress and the corresponding normal stress:

$$\boxed{\begin{aligned} \tau_1, \tau_2 &= \pm \sqrt{\left(\frac{\sigma_x - \sigma_y}{2}\right)^2 + \tau_{xy}^2} \\ \sigma &= \frac{\sigma_x + \sigma_y}{2} \end{aligned}} \quad (1.33)$$

In this case we see that on the face with maximum shear stress, the corresponding normal stress is not zero.

There are two main types of analyses that use these equations.

1. If we are only interested in finding the maximum stresses, and don't care about the corresponding orientation, then it is most convenient to use Eq. (1.31) and Eq. (1.33) directly.

2. If we need to visualize the stress element then the above approach is not the most helpful because with only those equations there is way to know which face corresponds to σ_1 and which to σ_2 , or to know what the direction of the max shear stress is. Instead, it is recommended to compute ϕ_p (Eq. (1.30)) then plug that angle into the transformation equations Eq. (1.29) to find the stress on that face. We would then need to use the transformation equations again for $\phi_p + 90^\circ$ (or use Eq. (1.31) to find the magnitude of the normal stress on the other face). If the maximum shear stress face is needed, the transformation equations should be used with $\phi_s = \phi_p + 45^\circ$. This procedure will allow one to determine the correct direction of the shear stress for the corresponding angle.

For the general 3-dimensional case it is easier to find principal stresses using an eigenanalysis. A principal stress will occur when the surface is aligned with the stress vector (i.e., there is no shear):

$$\mathbf{t} = \sigma_p \hat{\mathbf{n}} \quad (1.34)$$

for some scalar σ_p . This implies that

$$\mathbf{t} = [\boldsymbol{\sigma}] \hat{\mathbf{n}} = \sigma_p \hat{\mathbf{n}} \quad (1.35)$$

which is a standard eigenvalue problem. The principal stresses can be found by solving

$$|[\boldsymbol{\sigma}] - \sigma_p [\mathbf{I}]| = 0 \quad (1.36)$$

1.5.2 Mohr's Circle

It turns out that Eq. (1.29) defines an equation for a circle where the x, y axes correspond to σ and τ as shown in Fig. 1.12. The values for the center of the circle C and its radius R are shown in the figure. All possible stress states for the 2D case exist along the circle (changing ϕ). The principal stresses are the furthest points, on the circle, to the right and to the left. Geometrically it is clear to see that those locations correspond to $C \pm R$, which you can verify correspond to the equations for principal stresses. We see that the shear stress is zero at the principal stresses because Mohr's circle is always centered on the x -axis. Similarly, the maximum shear stresses will occur at the top and bottom of the circle (with a value equal to R), and we can see from the geometry that the normal stress is not zero at those locations.

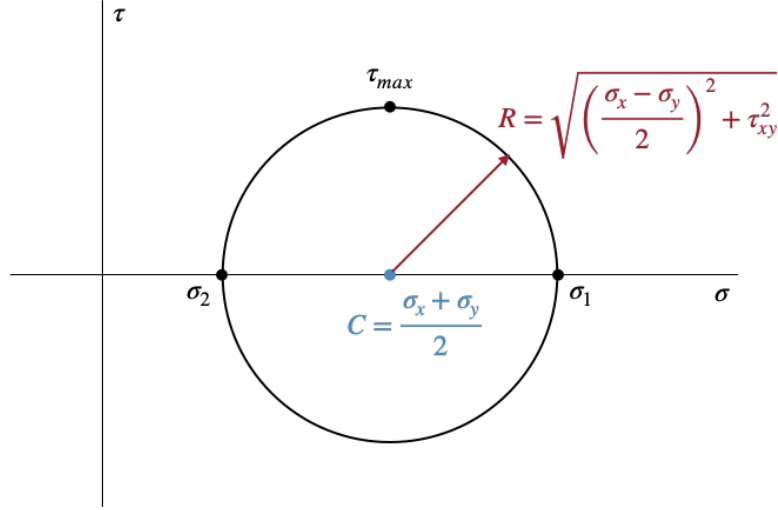


Figure 1.12: Depiction of Mohr's circle. All possibilities for the stress state occur along the circle.

Various rules exist to construct and interpret Mohr's circle as a function of ϕ . We will not discuss these as they just add extra complications and a conflicting sign convention. It is generally much easier just to use the transformation equations (Eq. (1.29)) or the maximum stress equations (Eqs. (1.31) and (1.33)). The main value for Mohr's circle is as a visualization aid, particularly in three-dimensions as we will see shortly.

Even in a biaxial stress state (i.e., plane stress, or what we've been looking at so far), it is important to remember that actual stress state is always three-dimensional. For example, we've considered a plane stress case with principal stresses σ_1 and σ_2 . This means that the out-of-plane principal stress, $\sigma_3 = 0$. Thus, the face containing σ_2 and σ_3 has its own Mohr's circle (the small circle in Fig. 1.13). Additionally, the face containing σ_1 and σ_3 has another Mohr's circle (the largest circle in Fig. 1.13). From this diagram we see that the maximum shear stress actually doesn't occur in the plane we were looking at (the circle between σ_1 and σ_2). But rather is given by:

$$\boxed{\tau_{max} = \frac{\sigma_1 - \sigma_3}{2}} \quad (1.37)$$

For many analyses we are most interested in the principal stresses and so this distinction is not important, but for cases where the maximum shear stress is an important value understanding this distinction is essential. We

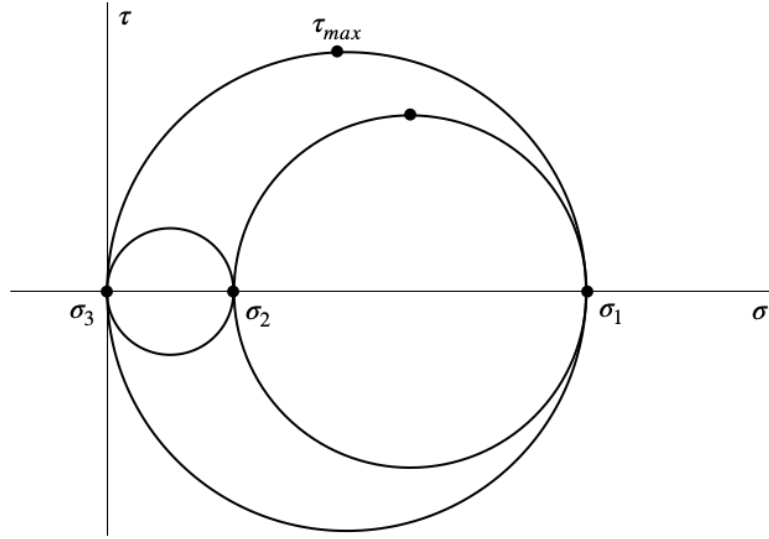


Figure 1.13: Three-dimensional Mohr's circle.

must take care to always evaluate the three-dimensional stress state.

In general, σ_3 need not be zero, it can be positive or negative (as can all principal stresses). By convention, the principal stresses are always ordered so that σ_1 is the largest, and σ_3 is the smallest. Using that convention, Eq. (1.37) is always true whereas Eq. (1.33) might not actually return the highest shear stress. Similarly, Eq. (1.31) might not actually return σ_1 and σ_2 if one or both are negative. That expression will return two of the principal stresses, and if the other is zero, all three should be reordered from largest to smallest to correspond to σ_1 , σ_2 , and σ_3 .

Chapter 2

Combined Loads

2.1 Axial Stress

An axial load along a beam generates a normal stress:

$$\sigma = \frac{F}{A} \quad (2.1)$$

where A is the cross-sectional area (see Fig. 2.1). This equation assumes that the beam is straight, homogenous, and that the force passes through the centroid of the cross-section. The stress profile is uniform along the cross-section as depicted in Fig. 2.2.

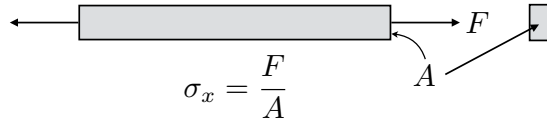


Figure 2.1: Depiction of axial stress.



Figure 2.2: An axial force creates a uniform stress profile across the cross section.

2.2 Bending Stress

If a bending moment exists, either from a transverse force or from a pure moment, the bending moment will produce bending stress in a beam. Figure 2.3 depicts a beam with a bending moment applied. The bending moment has a subscript z because the axis of the moment is in the z direction (out of the page). The pair of moments on either side of the beam must be in opposite directions for static equilibrium. The grid lines drawn across the beam are just for reference.

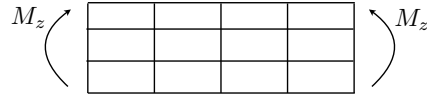


Figure 2.3: Depiction of a beam, under a bending moment, but without the deflection applied.

The bending moment will cause the horizontal lines to curve and the vertical lines to rotate (exaggerated in Fig. 2.4). We assume that the vertical lines rotate but remain straight, this assumption is usually referred to as: plane sections remain plane. You can see that the rectangles from the grid expand along the bottom of the beam and are thus in tension. Conversely, the grid on the top side of the beam contracts and is thus in compression. The direction of the bending moments can help you see which side is in tension and which is in compression. The side that the moment arrows “come out of” is in tension, and the side the arrows “go into” is in compression. Think of the curve from the moment arrows pulling from the bottom and pushing in the direction of the arrow.

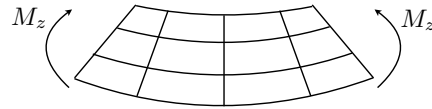


Figure 2.4: The bending moment causes a deformation of the structure, rotating vertical sections, and curving horizontal sections.

If the beam is expanded at the bottom and contracted at the top, then there must be a location somewhere between there where the length of the beam is unchanged. This location is called the neutral axis and is depicted as a dashed line in Fig. 2.5.

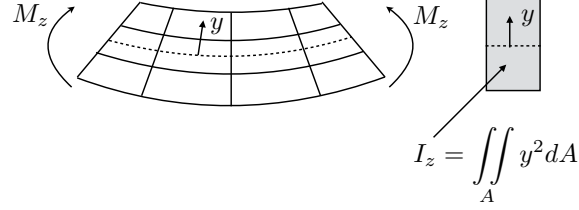


Figure 2.5: The dashed line corresponds to the neutral axis, and the moment of inertia is evaluated for the cross-section (depicted to the right).

To derive the bending stress formula we will examine an infinitesimal section of the beam (Fig. 2.6a). From geometry, we can say that the curvature of the beam (κ) is given by:

$$\kappa = \frac{1}{r} = \frac{d\phi}{ds} \quad (2.2)$$

The axial strain is how much a given section has elongated. We examine the strain at the blue cross section shown in Fig. 2.6a, which located at a distance y above the neutral axis.

$$\epsilon_x = \frac{L - L_0}{L_0} = \frac{(r - y)d\phi - ds}{ds} \quad (2.3)$$

Using the definition for curvature this expression simplifies to:

$$\epsilon_x = -\kappa y \quad (2.4)$$

If we assume that the axial stress is the only nonzero stress then:

$$\sigma_x = E\epsilon_x = -E\kappa y \quad (2.5)$$

The stress creates a force distribution across the cross section of $\sigma_x dA$. If we multiply that force by the moment arm (y) we get the local moment (Fig. 2.6b). Integrating across the face the moment from the stress distribution must equal the (negative of the) applied moment:

$$M_z = - \int_A y \sigma_x dA \quad (2.6)$$

Using Eq. (2.10) this expression becomes:

$$M_z = \int_A E \kappa y^2 dA \quad (2.7)$$

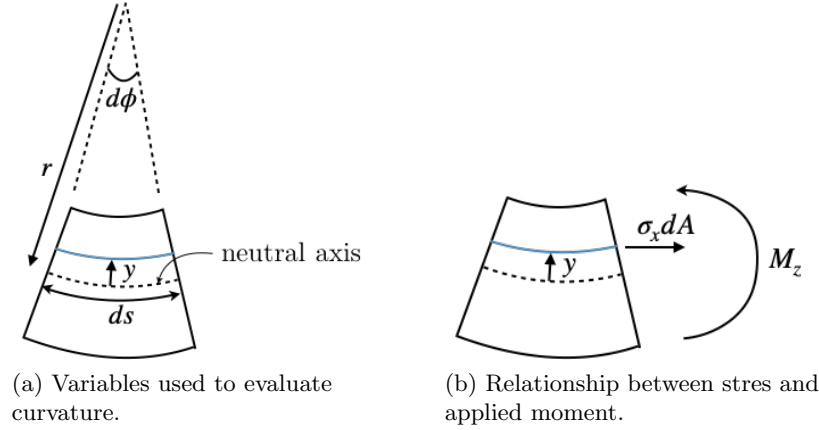


Figure 2.6: An infinitesimal section of a beam in bending.

For homogenous material E is constant. With our assumption that plane sections remain plane the curvature is also constant.

$$M_z = E\kappa \int_A y^2 dA \quad (2.8)$$

The remaining integral is called the *area moment of inertia* for the cross section:

$$I_z = \int_A y^2 dA \quad (2.9)$$

As we've seen, the value of y in the above integral is always measured relative to the neutral axis. The moment is thus given by:

$$M_z = E\kappa I_z \quad (2.10)$$

Finally, we combine this equation with Eq. (2.10) to give the *flexure formula*:

$$\sigma_x = -\frac{M_z y}{I_z} \quad (2.11)$$

Definitions for these values are seen in Fig. 2.7 with the beam on the left, and a view of the cross section on the right. Notice the two equivalent representations of a bending moment for the two coordinate systems. In one coordinate system we see a curved arrow. In the other, we see a double arrow. The relationship between them is given by the right hand rule: curve your right hand in the direction of the arrow and your thumb points in the direction of the moment (the double arrow).

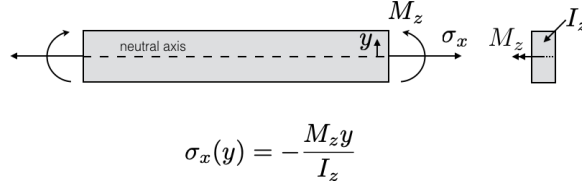


Figure 2.7: Definitions used in bending stress (flexure) formula. The rectangle to the right is the cross-section as viewed from the end of the beam.

Notice that the bending stress is a normal stress, and that it varies as a function of y . From the definition we can also see that the bending stress is zero at the neutral axis, and for this particular moment direction, is most negative at the top (compression), and most positive at the bottom (tension). This stress profile is visualized in Fig. 2.8, with compression at the top and tension at the bottom. Also, we note that bending stress can be decreased by increasing the moment of inertia.



Figure 2.8: Bending stress profile at a cross-section of the beam.

The subscripts and negative sign in the preceding equation are important if using a computational implementation. For hand calculations it is generally easier to determine the compression and tension side from observation. Furthermore, we are usually primarily interested in the maximum stress, which occurs at the furthest distance from the neutral axis. In this case, we drop the subscripts, and the sign, and use the following version:

$$\sigma_{max} = \frac{Mc}{I}$$

where c is the length from the neutral axis to the furthest point from the neutral axis.

2.2.1 Neutral Axis

Up to this point we have not defined where the neutral axis is actually located. All we have discussed is that the neutral axis does not contract or elongate. We can find its location by noting that our section is in pure

bending with no applied axial force. In other words, the placement of the neutral axis must be compatible with zero axial force. We saw already that the differential force at a given section is $dF = \sigma_x dA$, and the total force across the cross section is (using Eq. (2.10)):

$$\int_A dF = \int_A \sigma dA = -E\kappa \int_A y dA = 0 \Rightarrow \int_A y dA = 0 \quad (2.12)$$

Recall the definition of an area centroid relative to a given axis:

$$\bar{y} = \frac{\int_A y dA}{\int_A dA} \quad (2.13)$$

Comparing this equation to the one above, we see that the neutral axis is located at the y centroid of the cross-section. For simple cross sections the centroid can be found by inspection, but for more complex ones we may need to integrate.

2.2.2 Moments of Inertia

We saw that the definition for the moment of inertia was:

$$I = \int_A y^2 dA \quad (2.14)$$

However, most of the time we don't need to evaluate the integral and can use tabulated values for common cross-sectional shapes. A few common moments of inertia are listed below and are shown graphically in Fig. 2.9.

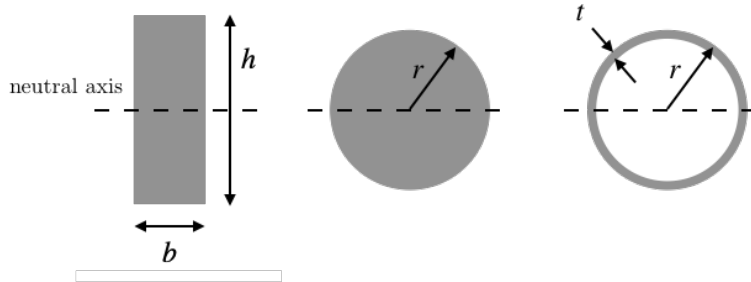


Figure 2.9: A rectangle, circle, and thin shell, whose moments of inertia are shown in this section.

A rectangle has a moment of inertia of about its neutral axis of:

$$\boxed{I = \frac{bh^3}{12}} \text{ (rectangle)} \quad (2.15)$$

where b is the dimension of the rectangle parallel to the neutral axis and h is the dimension perpendicular to the neutral axis.

A circle has a moment of inertia about its neutral axis of:

$$\boxed{I = \frac{\pi r^4}{4}} \text{ (circle)} \quad (2.16)$$

where r is the radius.

A thin circular shell (hollow circle where the thickness of the shell is small compared to its radius) has a moment of inertia about its neutral axis of (approximately):

$$\boxed{I = \pi r^3 t} \text{ (thin circular shell)} \quad (2.17)$$

where r is the mean radius, and t is the thickness of the shell. If the shell is thick, or higher accuracy is necessary, then one can just use formula for a solid circle and subtract out the moment of inertia of the missing interior.

Another useful concept in evaluating moments of inertia, without having to resort to the integral, is the parallel axis theorem. The parallel axis theorem allows us to compute the moment of inertia along any axis that is parallel to the centroidal axis. If I_c is the moment of inertia of some shape about its centroid, then referring to the nomenclature in Fig. 2.10, the moment of inertia about a parallel axis is given by:

$$I = I_c + Ad^2 \quad (2.18)$$

where A is the cross-sectional area.

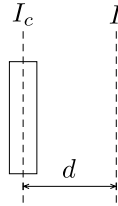


Figure 2.10: Figure used to demonstrate the parallel axis theorem.

2.2.3 Bidirectional Bending

If bending occurs in two planes the equation has an additional term

$$\sigma_x = -\frac{M_z y}{I_z} + \frac{M_y z}{I_y} \quad (2.19)$$

Like single directional bending it is often easier to determine the maximum stress locations from inspection rather than worry about the signs of the various terms. There are two common cases: a rectangular cross-section and a circular cross-section.

A rectangular cross-section with two moments is shown in the left frame of Fig. 2.11, where we are looking at the cut face. First, let's consider the moment pointing to the right. From the right hand rule we can see that the moment produces tension (red) at the top surface and compression (blue) at the bottom surface (see second pane). Similarly, the moment pointing upwards produces tension on the left side and compression on the right side (see third pane). If we superimpose both moments the maximum tension will be in the upper left corner (see last pane), and the maximum compression will be at the bottom right corner.

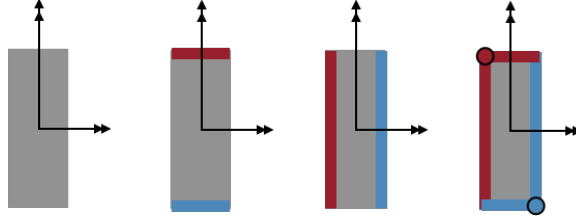


Figure 2.11: A rectangle in bidirectional bending will have maximum tensile and compressive stresses in the corners. Which corners are critical is determined from the directions of the moments using the right hand rule.

Now consider a circle with two moments as shown on the left side of Fig. 2.12. A circle is bit different because there are no corners so the same logic we used for the rectangle won't be enough. Instead, we combine the two moments vectorally (they are vectors). Now we can analyze the circle with one resultant moment using the same procedure we have been using previously, except that the coordinate system would need to be rotated to be aligned with the moment. In this case, we know that the maximum tension and compression will fall along a line perpendicular to the total moment. The max tension (red) and max compression (blue) are shown on

the right side of Fig. 2.12. The exact angle can be determined by knowing the magnitudes of the moments and the properties of vector summation. This same process works for a rectangle but it isn't as natural as the procedure shown previously.

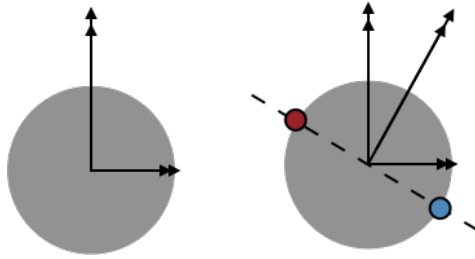


Figure 2.12: The moments acting on a circular cross section with bidirectional bending can be consolidated into a single moment, at which point the single directional bending procedure applies.

2.3 Direct Shear

Direct shear occurs when you have two equal and opposite forces that are essentially collinear (Fig. 2.13). If they are not collinear then the result would be bending, not shear. The equation for direct shear is:

$$\tau = \frac{V}{A}$$

This stress has a uniform distribution across the cross-section.

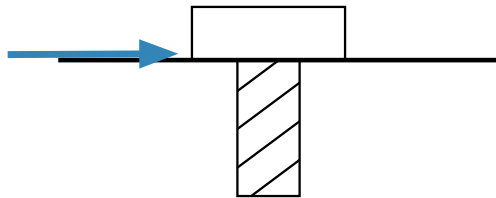


Figure 2.13: Direct shear of a bolt head.

2.4 Shear from Bending

Figure 2.14 shows a beam with a simple shear and bending moment diagram. If we isolate an element in the beam (also shown in the figure), we note that in general the bending moment will not be equal on both sides. Thus, a shear stress must exist in order for the element to be in static equilibrium. This stress is called *transverse shear stress*, or flexural shear stress. This shear stress is a result of bending.

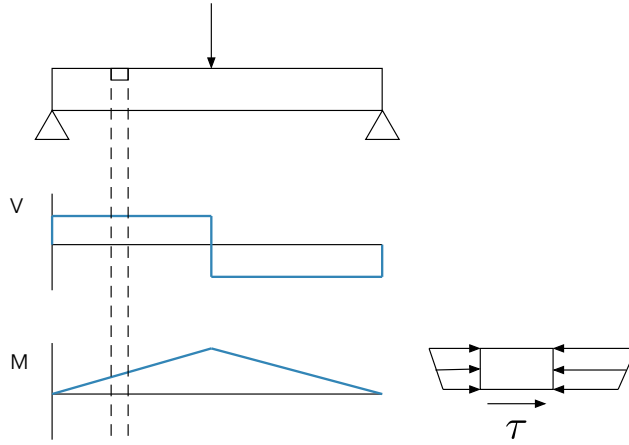


Figure 2.14: A beam under bending will also create shear stresses for static equilibrium. These shear stresses are called transverse shear.

Consider the beam shown in Fig. 2.15. Recall that the shear force (V) is related to the bending moment distribution by:

$$V = \frac{dM}{dx} \quad (2.20)$$

We omit the derivation of transverse shear stress, but the resulting shear stress is given by:

$$\tau = \frac{VQ}{It} \quad (2.21)$$

where V is the local shear force, I is the moment of inertia of the cross section, and t is the width of the cross-section as shown in Fig. 2.15.

One new quantity that arises in the derivation is the factor Q which is

given by the following integral:

$$Q = \int_y^c y' dA \quad (2.22)$$

Notice that the integral doesn't begin at the neutral axis, like the moment of inertia does, but rather begins at the point at which stress is evaluated at (y) and ends at the edge of the cross section (c) . In the above integral y' is just a dummy variable to distinguish between the variable y appearing in the limit.

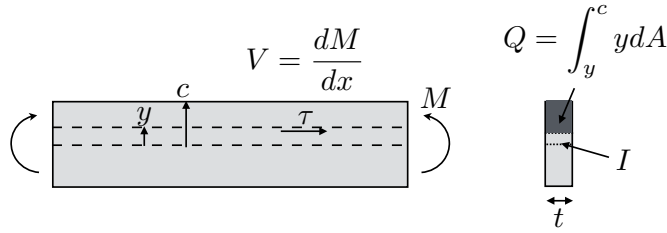


Figure 2.15:

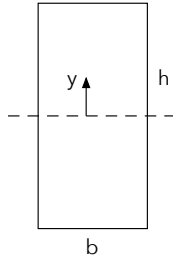


Figure 2.16: A rectangular cross section.

As an example, consider a rectangular section with base b and height h as shown in Fig. 2.16. The integral for Q , from generic point y , is given by:

$$Q = \int_y^c y' dA = b \int_y^{h/2} y' dy' = \frac{by'^2}{2} \Big|_y^{h/2} = \frac{b}{2} \left[\frac{h^2}{4} - y^2 \right] \quad (2.23)$$

and thus the shear stress for this section is:

$$\tau = \frac{V}{2I} \left(\frac{h^2}{4} - y^2 \right) \quad (2.24)$$

This shear stress profile is plotted in Fig. 2.17. Notice that it is zero at the ends and a maximum at the neutral axis. Keep in mind that this is a shear stress so the actual direction is in/out of the page, and not right/left as shown in the figure (the former is difficult to draw).



Figure 2.17: Stress profile for transverse shear. Note that this is a shear stress so the direction is in/out of the page.

From the definition of Q we can see that transverse shear stress is always zero at the top and bottom surfaces. The maximum shear is generally near the neutral axis where Q is largest, although that may vary somewhat if t is not constant for the cross-section.

Generally, it is the maximum shear stress that we are most concerned with. For common cross-sectional shapes the maximum shear stress is tabulated. This is particularly helpful because evaluating Q is a bit cumbersome. For a rectangular cross section the maximum shear stress is in the middle with a magnitude of:

$$\tau_{max} = \frac{3V}{2A} \quad (\text{rectangle}) \quad (2.25)$$

And for a circle the maximum shear stress is at the center with a magnitude of:

$$\tau_{max} = \frac{4V}{3A} \quad (\text{circle}) \quad (2.26)$$

The maximum transverse shear stress is generally located near the neutral axis, while the maximum bending (and torsional as will see) stresses are maximum at the furthest distance from the neutral axis. Thus, finding the most critical location often requires multiple evaluations. For long beams, the maximum bending stresses are much larger than transverse shear stresses, so because these stresses occur at different locations, transverse shear stress is not usually a limiting factor. However, for stout beams transverse shear stress may be more critical.

2.5 Torsion

A *torque* is a moment vector along the longitudinal axis of a shaft, which causes the structure to twist about that axis. A shaft that is twisted about

an axis is said to be in *torsion*. Some common examples include a screwdriver or a transmission shaft.

The derivation of shear stress for a shaft assumes that plane sections remain plane (i.e., no warping). This generally means that the cross-sections must be circular. For a circular shaft the torsion equation is:

$$\boxed{\tau_{x\theta} = \frac{Tr}{J}} \quad (2.27)$$

where T is the torque, r is the local radius, and J is the polar moment of inertia (see Fig. 2.18). Notice that there are two representations for torque, a double arrow or a curved arrow. The relationship between them is given by the right hand rule: curve your right hand in the direction of the curved arrow and your thumb points in the direction of the double arrow representation.

The polar moment of inertia is defined as:

$$J = \int r^2 dA \quad (2.28)$$

The polar moment of inertia for a solid circular section is:

$$\boxed{J = \frac{\pi R^4}{2}} \quad (2.29)$$

and for a hollow circular section is:

$$\boxed{J = \frac{\pi}{2}(R_o^4 - R_i^4)} \quad (2.30)$$

where R_i is the inner radius, and R_o the outer radius.

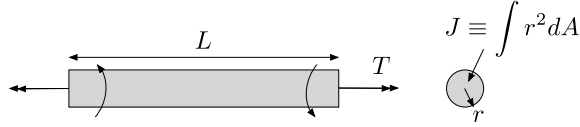


Figure 2.18: A torque causes torsional shear stress.

From the torsional stress equation (Eq. (2.27)) we see that the shear stress is zero at the center of the circular cross-section, and that increasing the polar moment of inertia reduces the maximum stress. From the equation for the polar moment of inertia of a circular section (Eq. (2.29)) we see that

the moment of inertia varies as R^4 . Because there is no stress in the center, a shaft can be made lighter with little to no penalty by making it hollow. Additionally, moving more material towards the outside will increase the polar moment of inertia and decrease torsional stress. This is why most drive shafts are hollow.

The profile for torsion is shown in Fig. 2.19 where we see that the torsional stress is zero in the center and maximum at the edge. Note that this is just a profile. The shear stress does not point left/right as depicted in the figure, but rather in/out of the page.



Figure 2.19: Stress profile for torsional shear stress.

As discussed, hollow circular sections are commonly used to carry torsional loads (Fig. 2.20). However, it is critical that the section is closed. For example, consider a thin shell circular section with a radius to thickness ratio of $r/t = 10$. If the section is not closed, then for a given torque the section will twist 300 X further than it will if the section is closed. Closed sections are essential for carrying torsional loads effectively.

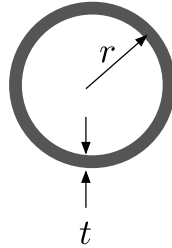


Figure 2.20: A hollow cross section commonly used to carry torsional loads.

While circular cross sections are most commonly used when torsion is involved, sometimes other cross sections are used. For rectangular cross sections an analytic solution does not exist, but approximate formulas do. Rectangular cross sections are not as effective in carrying torsional loads and often warp. For a rectangle with sides b and c , with b being the longer side, the maximum stress is located midway along b at the outer edge and is approximately:

$$\tau_{max} \approx \frac{T}{bc^2} \left(3 + \frac{1.8}{b/c} \right) \quad (2.31)$$

The stresses at the corners of the rectangle are zero.

2.6 Combined Loads

Most structures carry more than one of the stresses we have discussed in this chapter: axial, bending, flexural shear, and torsional. For a beam-like structure we can consider all possibilities by exploring forces in all three directions, and moments in all three directions. Figure 2.21 shows a structure, cut at some cross-section, with forces acting in all three axes. The yellow box represents an infinitesimal stress element on the front face of the structure. We are interested in determining the stresses acting on this element.

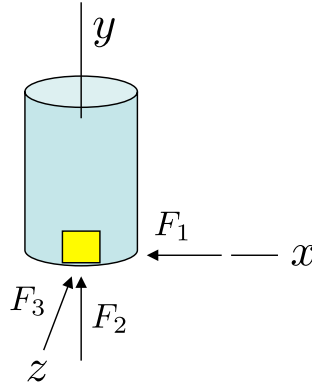


Figure 2.21: Forces acting in all axes at a cut face of some beam-like structure.

Let us now consider each of these forces one at a time:

- F_1 produces flexural shear (VQ/It). The force acts parallel to the bottom surface of A, and the shear stress on the bottom surface (where the cut face is) will be in the same direction as the force. This can be seen in Fig. 2.22.
- F_2 produces axial stress (F/A). This force is perpendicular to the cut face of element A, and in this case is compressive because it pushes into the face.
- F_3 does nothing to this particular stress element. This force pierces the element. The stress element is at the end (relative to F_3) where

Q , and thus the stress, goes to zero.

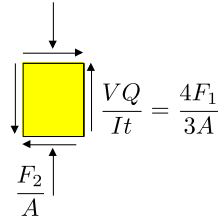


Figure 2.22: The resulting stresses on that stress element from the forces: F_1 , F_2 , and F_3 .

Let us now perform a similar analysis, but for the moments. Like before we consider moments acting in all three axes at the cut face of a structure, with a stress element on the front (Fig. 2.23).

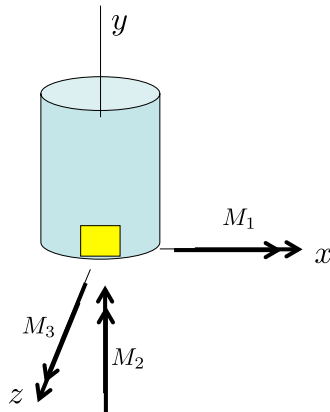


Figure 2.23: Moments acting in all axes at a cut face of some beam-like structure.

We consider each moment individually:

- M_1 creates bending stress (Mc/I). Based on the right-hand rule we can see that it produces tension (put thumb in direction of moment, if your fingers curl out of the element it is tension, if they curl in it is compression). This stress can be seen in Fig. 2.24.

- M_2 creates torsional shear stress (Tc/J). The direction is determined by the right hand rule (put thumb in direction of moment, the direction the fingers point when next to the element is the stress direction on that face). This is shown in Fig. 2.24.
- M_3 does not produce any stress on this particular moment, because the element is at the neutral axis for that particular bending stress.

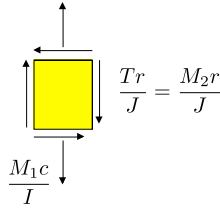


Figure 2.24: The resulting stresses on that stress element from the moments: M_1 , M_2 , and M_3 .

In general, both forces and moments exist and in that case the resulting stresses must be summed. For this example, with the directions shown, the resulting total stress from all three forces and moments is shown in Fig. 2.25.

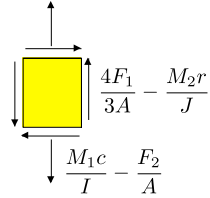


Figure 2.25: Total stresses from the three forces and three moments.

Visualizing the beam stresses resulting from these forces and moments takes some practice. Two-dimensional views, in particular, can make visualization difficult when starting out. To help, all four loading cases (axial, bending, transverse shear, and torsion) are visualized in Figs. 2.26 to 2.29 with an isometric view, a front view, a side view, and a view of the stress elements.

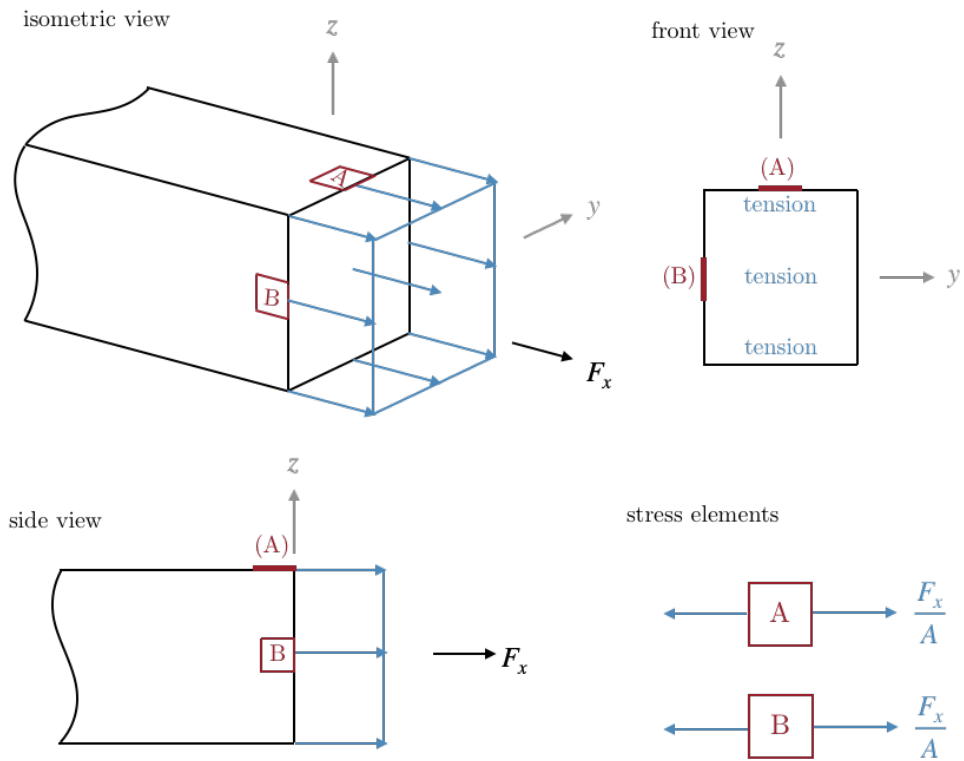


Figure 2.26: Normal stress distribution resulting from axial loading and the corresponding normal stresses on two stress elements.

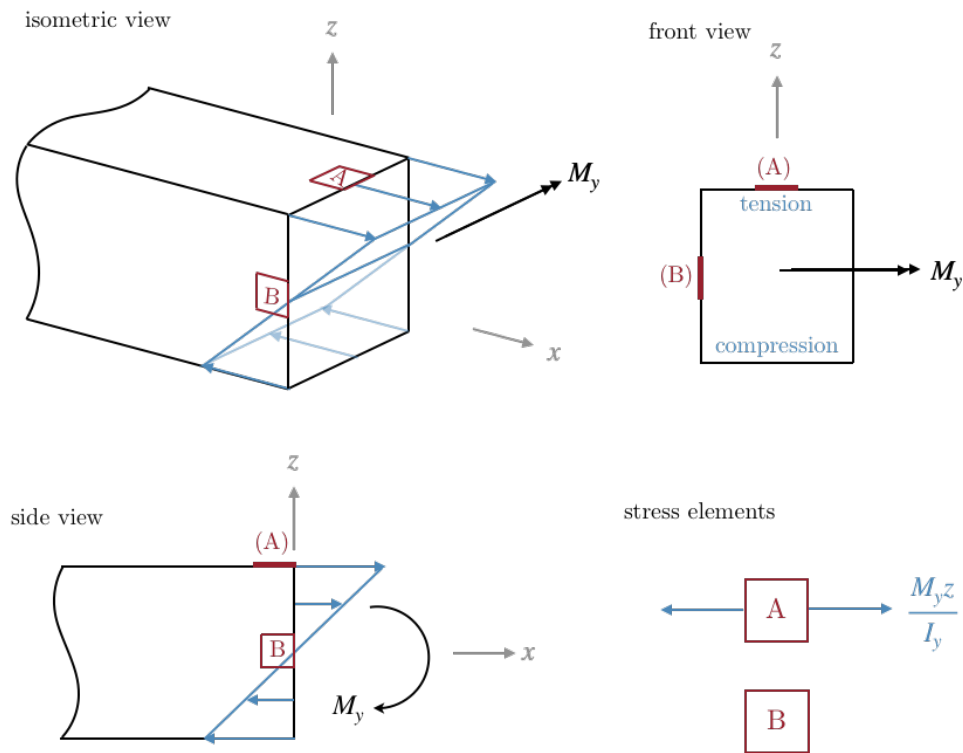


Figure 2.27: Normal stress distribution resulting from a bending moment and the corresponding normal stresses on two stress elements.

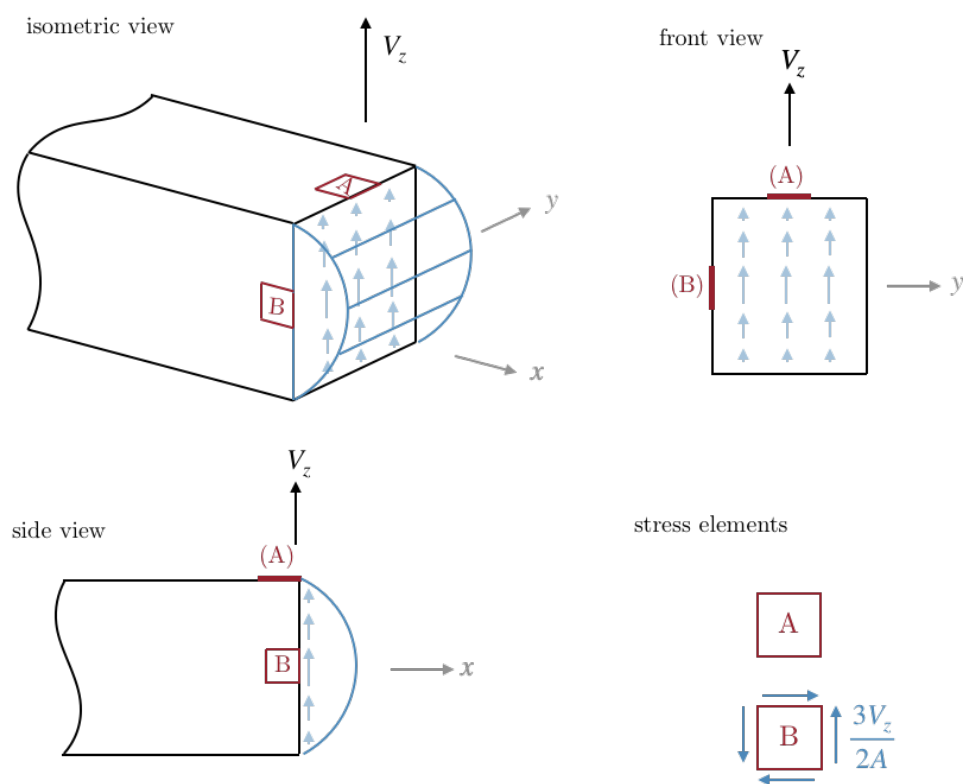


Figure 2.28: Shear stress distribution resulting from a transverse shear force and the corresponding shear stresses on two stress elements. The curved profile is meant to indicate the magnitude of the stress, whereas the arrows show direction (and their length helps indicate magnitude as well).

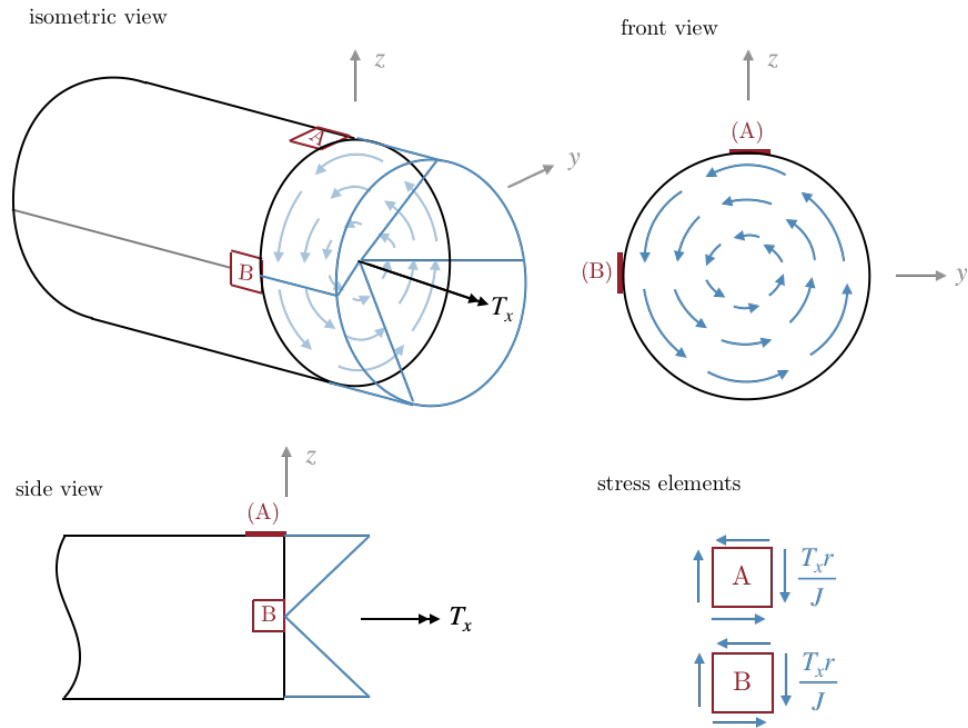


Figure 2.29: Shear stress distribution resulting from torsion and the corresponding shear stresses on two stress elements. The inverse conic profile is meant to indicate the magnitude of the stress, whereas the arrows show direction (and their length helps indicate magnitude as well).

2.7 Stress Concentrations

All of these analyses have assumed idealized material and geometric conditions. Real structures often contain discontinuities or irregularities in the materials and/or the geometry that cause local increases in stress. This localized stress increase is called a *stress concentration*. Some examples of features that cause stress concentrations are corners (which is why airplanes use rounded windows), holes, threads, grooves, etc.

For many canonical geometries, stress concentration factors are tabulated from experimental data. For example, consider the plate with a hole shown in Fig. 2.30. The stress near the hole is increased beyond what would be calculated by using $\sigma = F/A$, even accounting for the reduced cross-sectional area.



Figure 2.30: A plate with a hole experiences stress concentrations near the hole.

Stress concentration factors are typically of the form:

$$K = \frac{\sigma_{max}}{\sigma_0} \quad (2.32)$$

where K is the stress concentration factor, σ_{max} is the maximum stress experienced in the structure and σ_0 is the stress that would be predicted if no stress concentration existed. Thus, one can compute σ_0 using the standard methods discussed in this chapter, then multiply by the stress concentration factor K to determine the maximum stress that will be actually experienced.

An alternative approach is to use finite element methods. These methods are particularly helpful for more complex geometries that aren't available in tables.

Stress concentration factors are generally not applied for static loads with ductile materials, but are applied with brittle materials and dynamic loads (whether ductile or brittle). These scenarios are summarized in Table 2.1. The reason why stress concentration factors are not applied for ductile materials is because of [strain hardening](#). Stress concentration factors for dynamic loading will be discussed in a later chapter.

Table 2.1: Cases for which stress concentration factors are applied.

	Static Loads	Dynamic Loads
Ductile Material		X
Brittle Material	X	X

Chapter 3

Cylinders

3.1 Pressure Vessels

In Section 2.6 you may have found it surprising that even for a case with forces and moments in all directions, the resulting stress state had a normal stress in only one direction (see Fig. 2.25). In this chapter we will see that pressure vessels create normal stress in the other two directions (side to side and in/out of page).

Pressurized cylindrical structures are used in many applications such as pipes, storage tanks, spacecraft, submarines, etc. We will consider the cylinder whose cross section is shown in Fig. 3.1. The cylinder is hollow on the inside with an inner radius r_i and an outer radius r_o . In the general case there is a nonzero pressure on both the inside and outside of the cylinder. The pressure is a gauge pressure (i.e., relative to atmospheric). The outer pressure is usually zero (exposed to the atmosphere), but as we will see there are situations, like a cylinder inside a cylinder, that have external pressure so we will derive the general case.

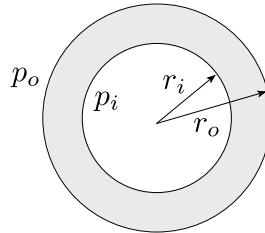


Figure 3.1: A pressurized cylindrical vessel with an inner and outer gauge pressure.

The derivation of the stresses created on a pressurized cylinder are contained in Appendix A. In this section we will just discuss the result. A pressurized cylinder experiences three normal stresses as shown in Fig. 3.2 with the cylinder side view on the left and the cross-sectional view on the right. A stress element in blue is shown on the outer edge of the cylinder. The stress σ_z is called the *longitudinal stress* or axial stress, and this stress is in the direction of the cylinder axis. This stress only exists if the ends of the cylinder are capped (i.e., not open to the atmosphere). The stress σ_θ is called the *hoop stress* or the *tangential stress* and this stress points along the circumference of the circle (forming a hoop). This is the largest stress for a pressure vessel. The stress σ_r is the radial stress. It points in the radial direction at each point in the cylinder. This is the smallest stress for a pressure vessel.

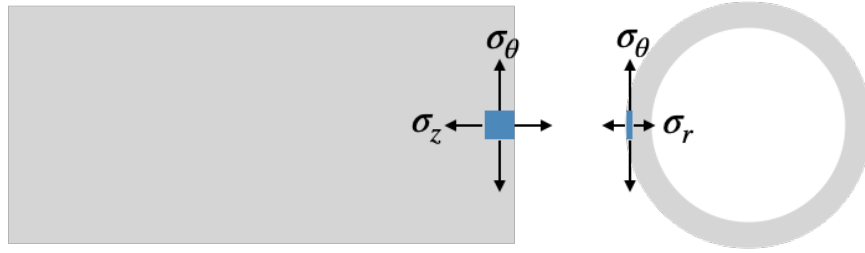


Figure 3.2: The stress components in a cylindrical pressure vessel.

The equation for these stresses are shown below.

$$\sigma_r = \frac{p_i r_i^2 - p_o r_o^2 + r_i^2 r_o^2 (p_o - p_i) / r^2}{r_o^2 - r_i^2} \quad (\text{radial}) \quad (3.1)$$

$$\sigma_\theta = \frac{p_i r_i^2 - p_o r_o^2 - r_i^2 r_o^2 (p_o - p_i) / r^2}{r_o^2 - r_i^2} \quad (\text{hoop}) \quad (3.2)$$

$$\sigma_z = \frac{p_i r_i^2 - p_o r_o^2}{r_o^2 - r_i^2} \quad (\text{longitudinal}) \quad (3.3)$$

Typically, there is no external pressure because the structure is in the surrounding atmosphere (i.e., $p_o = 0$). In that case, the equations simplify

to:

$$\sigma_r = -p_i \left(\frac{(r_o/r)^2 - 1}{(r_o/r_i)^2 - 1} \right) \quad (3.4)$$

$$\sigma_\theta = p_i \left(\frac{(r_o/r)^2 + 1}{(r_o/r_i)^2 - 1} \right) \quad (3.5)$$

$$\sigma_z = p_i \left(\frac{1}{(r_o/r_i)^2 - 1} \right) \quad (3.6)$$

For completeness, when $p_i = 0$ the equations simplify to:

$$\sigma_r = -p_o \left(\frac{1 - (r_i/r)^2}{1 - (r_i/r_o)^2} \right) \quad (3.7)$$

$$\sigma_\theta = -p_o \left(\frac{1 + (r_i/r)^2}{1 - (r_i/r_o)^2} \right) \quad (3.8)$$

$$\sigma_z = -p_o \left(\frac{1}{1 - (r_i/r_o)^2} \right) \quad (3.9)$$

Notice that the radial and hoop stresses are a function of r (varying between $r = r_i$ to $r = r_o$). These distributions are shown in Fig. 3.3 for the case with no external pressure. Notice that the radial stress is always compressive (negative) and that it varies from $-p$ on the inner surface to zero at the outer surface (or more generally it should match the inner and outer pressures at the inner and outer surface respectively). The radial stress as drawn in the figure depicts the distribution, not the direction of the stress.

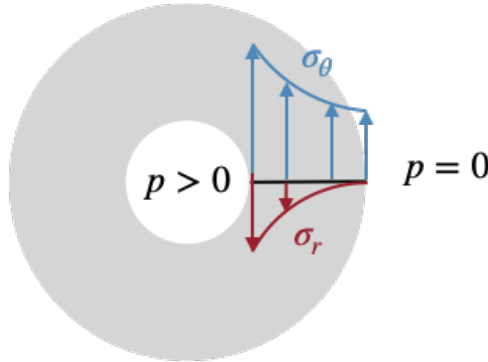


Figure 3.3: The distribution of hoop stress and radial stress for a cylinder with internal pressure.

The hoop stress is tensile (which should make sense for this case with pressure on the inside) and is largest at the inner surface. The hoop stress is always largest at the inner surface, and the maximum hoop stress is always larger than the maximum radial stress (although they approach the same value as the cylinder becomes infinitely thick). If longitudinal stress exists, its magnitude is between the hoop and radial stresses.

The hoop, longitudinal, and radial stresses are principal stresses with magnitudes descending in that order. Thus, the maximum shear stress is typically:

$$\frac{\sigma_\theta - \sigma_r}{2} \quad (3.10)$$

unless one of the ends is not capped. For a non-capped pressure vessel, $\sigma_z = 0$, and that stress could then be one of the largest/smallest stresses.

3.2 Thin Pressure Vessel

A cylinder can be considered a thin shell when the thickness is less than 10% of the radius ($t/r < 0.1$). In this case, the radial stress is very small and is considered negligible. In the limit that $r \gg t$ we can derive expression for the hoop and longitudinal stress from a force balance as depicted in Fig. 3.4

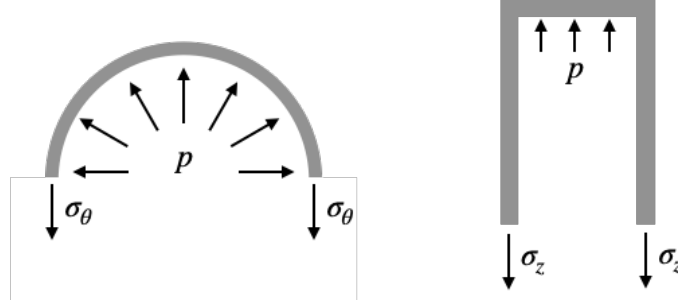


Figure 3.4: A thin shell cylinder with a cross-sectional cut away view on the left, and a side cut away view on the right.

For the hoop stress force balance we have:

$$2\sigma_\theta 2tL = pdL \Rightarrow \sigma_\theta = \frac{pd}{2t} \quad (3.11)$$

where L is the length, or height, of the cylinder into the page. For longitudinal stress the force balance gives:

$$\sigma_z \pi dt = p\pi \frac{d^2}{4} \Rightarrow \sigma_z = \frac{pd}{4t} \quad (3.12)$$

To summarize, for a thin cylindrical shell with internal pressure, the stresses are:

$$\sigma_r = 0 \quad (3.13)$$

$$\sigma_\theta = \frac{pr}{t} \quad (3.14)$$

$$\sigma_z = \frac{pr}{2t} \quad (3.15)$$

Notice that the hoop stress is twice that of the longitudinal stress. This is why long pressurized tubes split along the length, and not along a cross-section. You may have observed this behavior with a garden hose, for example.

3.3 Press/Shrink Fits

Consider two cylinders where the inner cylinder has an outer radius larger than the outer cylinder's inner radius (Fig. 3.5). The two cylinders can be put together either through force (a press fit) or by heating the outer cylinder then sliding them together and letting it shrink on (shrink fit). In either case, the interference causes a pressure between the two cylinders. That pressure can be computed as¹:

$$p = \frac{E\delta}{2R^3} \left[\frac{(r_o^2 - R^2)(R^2 - r_i^2)}{r_o^2 - r_i^2} \right] \quad (3.16)$$

where δ is the *radial interference*: the outer radius of inner cylinder (minus) inner radius of outer cylinder. The radius R is the nominal radius between the two cylinders. We can estimate the pressure for a situation where the two cylinders are made of different materials, although the formula is more complex:

$$p = \frac{\delta}{R \left[\frac{1}{E_o} \left(\frac{r_o^2 + R^2}{r_o^2 - R^2} + \nu_o \right) + \frac{1}{E_i} \left(\frac{R^2 + r_i^2}{R^2 - r_i^2} - \nu_i \right) \right]} \quad (3.17)$$

A press/shrink fit can be analyzed by breaking it down into two separate problems. The inner cylinder experiences an external pressure, and the outer cylinder experiences an internal pressure (Fig. 3.6), with the pressure given by the equations above. From the discussion of last section, we already know how to solve both of these problems. The result is a hoop stress profile like that shown in Fig. 3.7. Notice that the inner cylinder experiences a compressive hoop stress, while the outer cylinder experiences a tensile hoop stress.

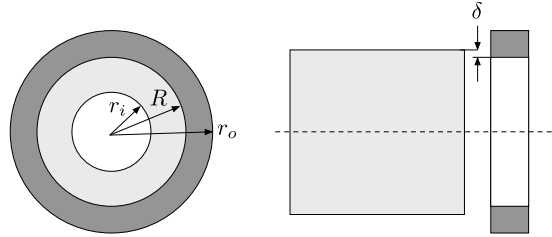


Figure 3.5: A shrink fit or press fit where the inner cylinder's outer diameter is slightly larger than the outer cylinder's inner diameter.

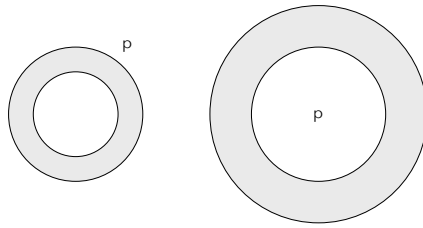


Figure 3.6: The press/shrink fit can be considered as two problems: the inner cylinder has an external pressure while the outer cylinder has an internal pressure.

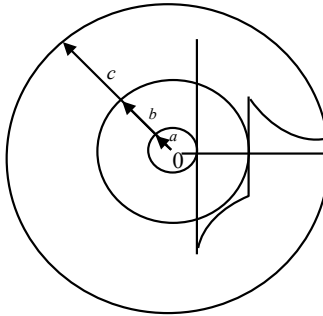


Figure 3.7: The hoop stress profile for a press/shrink fit. Compressive hoop stress on the inner cylinder and tensile hoop stress on the outer cylinder.

As a final complication, the press/shrink fit cylinders may be pressurized on the inside as depicted in Fig. 3.8. In fact, this is the primary motivation for a press/shrink fit. As we will see the press/shrink fit allows us to carry higher internal pressures before failure. An example is a gun barrel that is made from a press fit, and when fired, carries an internal pressure inside the barrel.

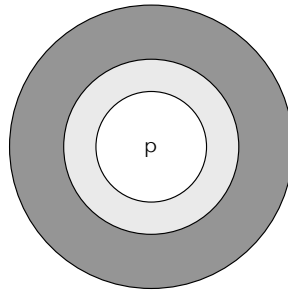


Figure 3.8: A press/shrink fit with internal pressure.

If we assume linearly elastic materials, then the deflections, and thus strain and stress can be superimposed. The way to solve this problem then is as depicted in Fig. 3.9. We solve for the stress distribution on the press/shrink fit cylinder with zero pressure on the inside. We then solve for the stress distribution on a thick cylinder (considering the press/shrink fit as one thick cylinder) with an internal pressure. Both of these scenarios we already know how to analyze. Finally, we simply add these stress distributions together to get the total stress for a press fit with internal pressure. This principle of superposition works because we have assumed linearly elastic materials.

Examining Fig. 3.9 we can see that, for the interior cylinder, the compressive hoop stress partially negates the tensile compressive stress from the internal pressure. Because the inner surface is most critical, this allows the structure to carry more pressure before reaching critical stress. This ability to carry a higher pressure is the motivation for a press/shrink fit. The critical locations are both of the interior surfaces (interior of inner cylinder and interior of outer cylinder). We won't know beforehand, which surface is more critical without computing the stresses at both locations. In this example, the outer cylinder has a larger hoop stress. In an optimal design, the structure is utilized most efficiently if both surfaces are designed to fail at the same time.

¹Budynas, R. G., Advanced Strength and Applied Stress Analysis, McGraw-Hill, 1999.

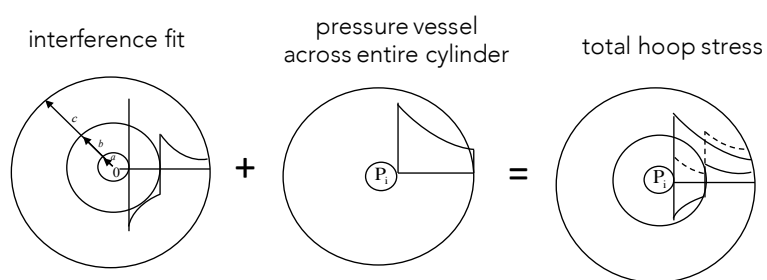


Figure 3.9: A press/shrink fit with internal pressure is analyzed as the superposition of a press/shrink fit with no pressure and a solid cylinder with internal pressure.

Chapter 4

Deflection

Deflections are fundamental in structural analysis. They are bit more difficult to compute using analytic approaches as compared to stresses. In this chapter we will study one energy method based on Castigliano's second theorem.

4.1 Strain Energy

Consider a general, undeformed, elastic structure subjected to applied loads. The first law of thermodynamics states that:

$$W + Q = T + U \quad (4.1)$$

where W is the work done by the applied loads, Q is the heat absorbed by the structure from its surroundings, T is a change in kinetic energy, and U is the change in internal energy. For a structure we can usually assume that the deformation process is adiabatic ($Q = 0$) and that the loads are applied slowly enough such that static equilibrium is maintained ($T = 0$). In that case we have:

$$W = U \quad (4.2)$$

which states that the mechanical work done by the applied loads is equal to the change in the internal energy of the structure. If the material is elastic then all of that internal energy could be recovered when the loads are removed. This energy being stored in the deformed structure is called the *strain energy*.

Consider a differential volume with stress in one direction (σ_x) as shown in Fig. 4.1. The work associated with the deformation is the force ($\sigma_x dydz$)

times the elongation ($d\epsilon_{xx}dx$). Thus, the strain energy from this element with stress in one direction is:

$$dU = \int_0^{\epsilon_{xx}} \sigma_{xx} d\epsilon_{xx} dx dy dz = \int_0^{\epsilon_{xx}} \sigma_{xx} d\epsilon_{xx} dV \quad (4.3)$$

The strain energy in the entire structure is then integrated across the entire volume:

$$U = \int_V \left(\int_0^{\epsilon_{xx}} \sigma_{xx} d\epsilon_{xx} \right) dV \quad (4.4)$$

A three-dimensional stress state follows the same form, we just add up all the strain energies from each stress times its corresponding strain.

$$U = \int_V \left(\int_0^{\epsilon_{ij}} \sigma_{ij} d\epsilon_{ij} \right) dV \quad (4.5)$$

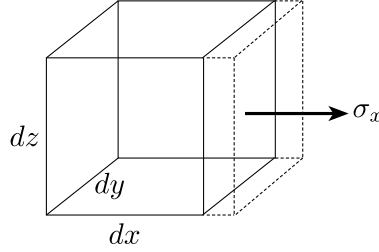


Figure 4.1: A differential volume with stress applied in one direction showing the corresponding deformation.

For example, consider an axial loaded bar as shown in Fig. 4.2. If the material is isotropic and linearly elastic, and no other stress components

exist, then $\epsilon = \sigma/E$ and $d\epsilon = d\sigma/E$. Then the strain energy is:

$$U = \int_V \left(\int \sigma d\epsilon \right) dV \quad (4.6)$$

$$U = \int_V \left(\int \sigma \frac{d\sigma}{E} \right) dV \quad (4.7)$$

$$U = \int_V \frac{\sigma^2}{2E} dV \quad (4.8)$$

$$U = \int_V \frac{F^2}{2EA^2} dV \quad (4.9)$$

$$U = \int_0^L \frac{F^2}{2EA^2} A dx \quad (4.10)$$

$$U = \int_0^L \frac{F^2}{2EA} dx \quad (4.11)$$

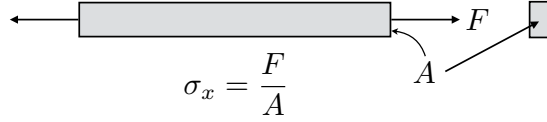


Figure 4.2: A bar loaded with an axial force.

Many mechanical structures can be represented by beams, and using a similar process we can determine the strain energy associated with axial loading, bending, transverse shear, and torsion.

As we just derived, axial loading has an associated strain energy of:

$$U = \int \frac{F^2}{2EA} dx \quad (4.12)$$

Bending has a strain energy of:

$$U = \int \frac{M^2}{2EI} dx \quad (4.13)$$

Transverse shear has a strain energy of:

$$U = \int \frac{CV^2}{2AG} dx \quad (4.14)$$

where the constant C is an empirical constant depending on the cross-section. For typical geometries and loads, the strain energy associated with transverse shear is negligible compared to that of bending and so we generally omit it. For curved beams or for very short beams including the strain energy from transverse shear can be important. Torsion has a strain energy of:

$$U = \int \frac{T^2}{2GJ} dx \quad (4.15)$$

4.2 Castigliano's Theorems

While the discussion so far has been primarily theoretical, there are many practical applications built around energy methods. In this chapter we will learn an application that will allow us to predict deflections.

The principle of minimum potential energy states that of all displacement fields that satisfy the equations of equilibrium, the correct state is the one that makes the total potential energy of the structure a minimum. This principle leads to Castigliano's first theorem. We won't discuss this theorem as we are primarily interested in the second theorem.

The principle of minimum *complementary* energy states that of all the states of stress which satisfy the equations of equilibrium, the correct state is that which makes the total *complementary* energy of the structure a minimum. Complementary energy (C) is depicted in Fig. 4.3. For linear elastic structures $U = C$ and we will assume linear elastic structures in this chapter.

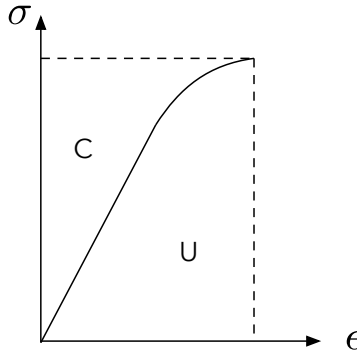


Figure 4.3: A graphical depiction of strain energy U and complimentary energy C .

Mathematically, Castigliano's second theorem is expressed as:

$$q_i = \frac{\partial C}{\partial Q_i} \quad (4.16)$$

or for a linear elastic structure:

$$q_i = \frac{\partial U}{\partial Q_i} \quad (4.17)$$

In this equation q_i is a generalized displacement, and Q_i is a generalized force in the direction of q_i . To make this more concrete, if $Q = F$ was a force applied in the x direction then the corresponding generalized displacement would be x . Or if $Q = M$ was a moment then the corresponding generalized displacement would be θ in the direction of positive M . In other words, Q represents some force or moment and q represents the corresponding linear or angular displacement in the direction of positive Q .

We can now apply this theorem to the strain energy expressions we derived earlier. It is generally easiest to apply the derivative inside of the integral rather than computing the strain energy first. This yields the equations below, which can be used to determine deflections:

For axial loading:

$$q_i = \int \frac{F}{EA} \frac{\partial F}{\partial Q_i} dx \quad (4.18)$$

For bending:

$$q_i = \int \frac{M}{EI} \frac{\partial M}{\partial Q_i} dx \quad (4.19)$$

For torsion:

$$q_i = \int \frac{T}{GJ} \frac{\partial T}{\partial Q_i} dx \quad (4.20)$$

4.2.1 Existing Loads

The preceding discussion is rather abstract, so let's consider an example. Consider a cantilevered beam with a point load at the end. We are interested in the deflection at the end of the beam (and in the direction of P). In this case our generalized force is P and the corresponding generalized deflection, let's call it y , is what we want to solve for.

This problem only has bending loads (ignoring transverse shear as is typical) so we will use the expression (Eq. (4.19)):

$$y = \int_0^L \frac{M}{EI} \frac{\partial M}{\partial P} dx \quad (4.21)$$

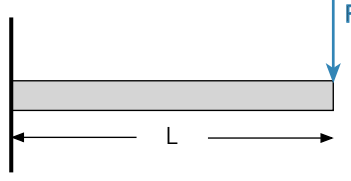


Figure 4.4: A cantilevered beam with a point load at the end.

We now need to get an expression for M as a function of x , which is the dimension along the beam. Both E and I are constant along the beam. We are free to define x from any direction that we like. We will cut the beam at some arbitrary section from the free end as shown in Fig. 4.5.

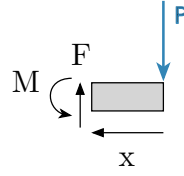


Figure 4.5: A cut section in the beam to analyze the internal moment.

The shear force equals P , but we will neglect deflection due to shear. As discussed earlier its contribution is generally negligible for deflection. A moment balance gives:

$$M = Px \quad (4.22)$$

using the directions defined. This equation defines the moment distribution as a function of x . As a sanity check we can see that at $x = 0$ (the free end) the moment is zero, which is correct, and at the wall $M = PL$, which is also correct. The formula also asks for the partial derivative:

$$\frac{\partial M}{\partial P} = x \quad (4.23)$$

We now plug these two equations into our deflection equation and integrate

from $x = 0$ to $x = L$:

$$y = \int_0^L \frac{Px}{EI}(x)dx \quad (4.24)$$

$$= \frac{P}{EI} \int_0^L x^2 dx \quad (4.25)$$

$$= \frac{P}{EI} \frac{L^3}{3} \quad (4.26)$$

This procedure correctly produced the known solution for the deflection of a cantilever beam with a point load at the end.

4.2.2 Dummy Loads

This theorem can also be applied to find deflections at locations where no load exists. The procedure there is to compute the strain energy as if the fictitious load existed, take derivatives as needed, then set the fictitious load to zero. In other words:

$$q = \frac{\partial U}{\partial Q} \bigg|_{Q=0} \quad (4.27)$$

For example, consider the simply supported beam shown in Fig. 4.6. We may be interested in the deflection at the midpoint of the beam, but no force exists there so we cannot apply Castigliano's formula. The approach to solve this is to first add a dummy force in the middle, which we will call Q . We then proceed as we would normally.

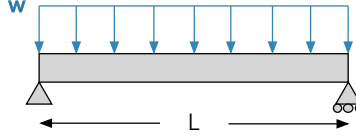


Figure 4.6: A simply supported beam with a distributed load.

First, we find the reaction forces as shown in Fig. 4.7. Next, we need to find a general expression for the shear and bending moment within the beam. We will examine a cut section as shown in Fig. 4.8. In this case we will ignore the contribution of shear to the deflection as it is generally negligible. From a force balance, the moment is given by:

$$M = \left(\frac{wL}{2} + \frac{Q}{2} \right) x - w \frac{x^2}{2} \quad (4.28)$$

Castigliano's theorem then requires the partial derivative:

$$\frac{\partial M}{\partial Q} = \frac{x}{2} \quad (4.29)$$

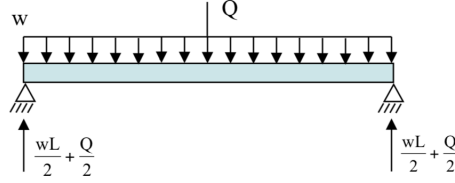


Figure 4.7: Reaction forces for distributed load with point load in center.

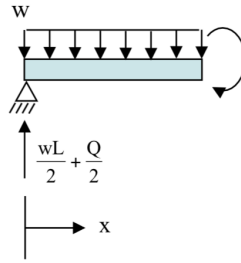


Figure 4.8: A cut section to find the internal moments of the beam.

We now have the pieces we need to put the integral together. We need to integrate over the entire structure, not just to the point of interest. We only computed the moment for half of the beam, but we know from symmetry that the other side will contribute the same amount to the deflection. Thus, we only need to integrate over half of the beam then multiply by 2.

$$y = 2 \int_0^{L/2} \frac{M}{EI} \frac{\partial M}{\partial Q} dx \quad (4.30)$$

$$= \frac{2}{EI} \int_0^{L/2} \left[\left(\frac{wL}{2} + \frac{Q}{2} \right) \frac{x^2}{2} - w \frac{x^3}{4} \right] dx \quad (4.31)$$

$$(4.32)$$

Recall that Q was really a fictitious point. At some point we need to set $Q = 0$. We can do it at the very end, although it will be easier to do it now rather than keep it around through all the integration. The dummy

variable can be eliminated at any point once the partial derivative is taken. Setting $Q = 0$ and integrating gives:

$$y = \frac{2}{EI} \int_0^{L/2} \left[\frac{wLx^2}{4} - w\frac{x^3}{4} \right] dx \quad (4.33)$$

$$= \frac{w}{2EI} \int_0^{L/2} (Lx^2 - x^3) dx \quad (4.34)$$

$$= \frac{w}{2EI} \left(L\frac{x^3}{3} - \frac{x^4}{4} \right)_0^{L/2} \quad (4.35)$$

$$= \frac{w}{2EI} \left(\frac{L^4}{24} - \frac{L^4}{64} \right) \quad (4.36)$$

$$= \frac{wL^4}{76.8EI} \quad (4.37)$$

The value for this deflection is positive meaning its direction is downward, in the positive direction of Q .

4.2.3 Statically Indeterminate Structures

Castigliano's theorem is also useful in solving statically indeterminate structures. Consider the structure shown in Fig. 4.9a (the circle is another representation of a roller pin joint). A free body diagram of the system is seen in Fig. 4.9b. A force balance yields:

$$R_A + R_B - P = 0 \quad (4.38)$$

while a moment balance at the wall yields:

$$M_A - \frac{PL}{2} + R_B L = 0 \quad (4.39)$$

Unfortunately there are three unknown reactions (R_A, R_B, M_A), but only two equations. This is an example of a *statically indeterminate* structure. That means the equations of static equilibrium are insufficient to analyze the structure.

One approach to obtaining a third equation is to use Castigliano's theorem. We know, for example, that the vertical deflection at B is zero. There is already a load there (R_B) so we can apply the theorem and set the deflection to zero:

$$0 = \int \frac{M}{EI} \frac{\partial M}{\partial R_B} dx \quad (4.40)$$

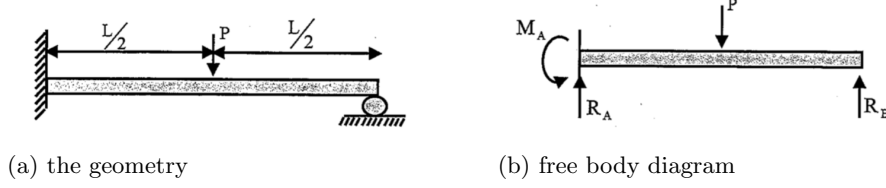


Figure 4.9: A cantilevered beam resting on a roller pin joint with a force in the middle.

This gives us a third equation for the three unknowns allowing us to solve the system.

We now need to compute the moment throughout the structure. However, because of the point load in the middle we need to express the moment piecewise (separate expressions for the two halves). Let us define x as starting from the right side of the beam. Then for the right half of the beam we have:

$$M = R_B x \quad (4.41)$$

and

$$\frac{\partial M}{\partial R_B} = x \quad (4.42)$$

For the left half we have:

$$M = R_B x - P(x - L/2) \quad (4.43)$$

and

$$\frac{\partial M}{\partial R_B} = x \quad (4.44)$$

If we put all this together we have the following expression:

$$0 = \int_0^{L/2} \frac{R_B x^2}{EI} dx + \int_{L/2}^L \frac{R_B x^2 - P x^2 + \frac{PLx}{2}}{EI} dx \quad (4.45)$$

This equation can be integrated and solved for R_B (note that it is the only unknown in the expression). The math is a bit tedious so we will omit it here, but the result is:

$$R_B = \frac{5}{16} P \quad (4.46)$$

We now can solve Eqs. (4.38) and (4.39) for the remaining reactions.

Chapter 5

Static Failure

Static failure theories are not derived from fundamental equations, but rather are semi-empirical models based on experiments and reasoning. There are two major categories: failure theories for ductile materials and failure theories for brittle materials. We only discuss failure theories for ductile materials in this chapter (although the last method is also used for brittle materials). Three such theories will be introduced.

5.1 Maximum Shear Stress Theory

Maximum shear stress (MSS) theory, also known as *Tresca theory* is based on the concept of maximum shear stress and experimental data for tension tests. Consider a bar loaded axially in tension (Fig. 5.1).

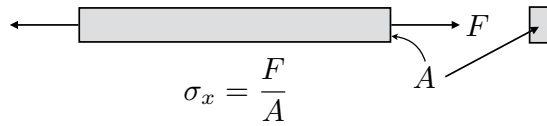


Figure 5.1: A bar loaded in tension.

For a simple tension test the stress is $\sigma = F/A$ and the bar will yield once σ reaches σ_y . The corresponding maximum shear stress for this scenario is $\tau_{crit} = \sigma_y/2$ (think of the corresponding Mohr's circle with $\sigma_1 = \sigma_y, \sigma_2 = 0, \sigma_3 = 0$). MSS theory predicts that a general specimen will yield once its maximum shear stress reaches this value ($\sigma_y/2$). Recall that the maximum shear stress for a general stress element is $\tau_{max} = (\sigma_1 - \sigma_3)/2$ (see Eq. (1.37)).

Thus, MSS predicts failure for a general element when:

$$\tau_{max} \geq \tau_{crit} \quad (5.1)$$

$$\frac{\sigma_1 - \sigma_3}{2} \geq \frac{\sigma_y}{2} \quad (5.2)$$

$$\Rightarrow \sigma_1 - \sigma_3 \geq \sigma_y \quad (5.3)$$

For design purposes we typically include a safety factor (n). The magnitude of the safety factor tells us how far we are from failure. For example, a value of 1 means we are right at the failure point, whereas value of 1.2 means we have a 20% margin against failure. Including the safety factor gives the following failure criteria written in terms of the maximum shear stress:

$$\tau_{max} = \frac{\sigma_y}{2n} \quad (5.4)$$

or in terms of the principal stresses:

$$\sigma_1 - \sigma_3 = \frac{\sigma_y}{n} \quad (5.5)$$

We have implicitly used this failure theory in some of our problems where we have constrained the maximum shear stress.

For a plane stress scenario we can visualize the stress envelope for MSS theory as shown in Fig. 5.2. Everything in blue is safe, while any stress state outside of the blue area would fail according to the MSS criteria.

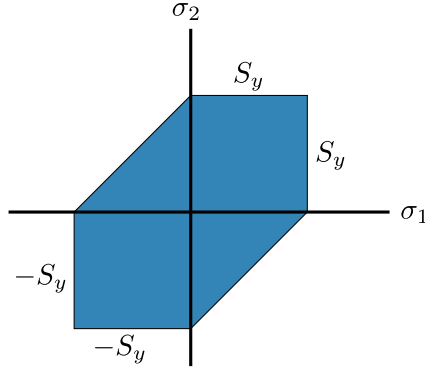


Figure 5.2: Failure envelope for MSS theory.

5.2 Distortion Energy Theory

The MSS theory is straightforward to apply, but is often overly conservative. The distortion energy theory, discussed in this section, is more accurate and thus the MSS theory is not typically used anymore.

The motivation for the theory comes from the observation that a ductile material under hydrostatic stress (equal stress on all sides) is able to carry much higher loads before failure than it can in uniaxial loading. It is hypothesized that yielding is not caused by tension or compression per se, but rather by the angular distortion of the element.

Conceptually we could decompose any triaxial stress state (seen on the left in Fig. 5.3) into a hydrostatic component + a distortional component. The hydrostatic component would just be given by the average of the principal stresses:

$$\sigma_{avg} = \frac{\sigma_1 + \sigma_2 + \sigma_3}{3} \quad (5.6)$$

The theory suggests that the energy in the remaining distortional state is the important factor in predicting yielding.

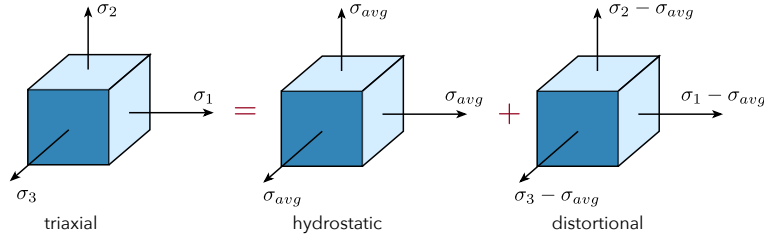


Figure 5.3: A general stress state can be decomposed into the sum of an average stress and a distortional component.

Strain energy was discussed previously in Chapter 4. The strain energy (per unit volume) associated with the general triaxial stress state is:

$$u = \frac{1}{2} [\epsilon_1 \sigma_1 + \epsilon_2 \sigma_2 + \epsilon_3 \sigma_3] \quad (5.7)$$

If we substitute in the stress/strain relationships for an isotropic material (Eq. (1.16)) we get:

$$u = \frac{1}{2E} [\sigma_1^2 + \sigma_2^2 + \sigma_3^2 - 2\nu(\sigma_1 \sigma_2 + \sigma_2 \sigma_3 + \sigma_3 \sigma_1)] \quad (5.8)$$

The strain energy for the hydrostatic case would then be:

$$u_h = \frac{3\sigma_{avg}^2}{2E}(1 - 2\nu) \quad (5.9)$$

If we substitute in the formula for σ_{avg} (Eq. (5.6)) we get:

$$u_h = \frac{1 - 2\nu}{6E}(\sigma_1^2 + \sigma_2^2 + \sigma_3^2 + 2\sigma_1\sigma_2 + 2\sigma_2\sigma_3 + 2\sigma_3\sigma_1) \quad (5.10)$$

Now, we can compute the distortion energy as the difference between these two energies:

$$u_d = u - u_h = \frac{1 + \nu}{3E} \left[\frac{(\sigma_1 - \sigma_2)^2 + (\sigma_2 - \sigma_3)^2 + (\sigma_3 - \sigma_1)^2}{2} \right] \quad (5.11)$$

Note that the distortion energy is zero if all principal stresses are equal as expected.

The distortion energy theorem predicts yielding when the distortion energy in a general stress element equals the distortion energy required for a bar in a tensile test to yield (very similar to the previous case). For a 1D axial loaded tensile test there is only one principal stress and if it is at its failure point then: $\sigma_1 = \sigma_y, \sigma_2 = 0, \sigma_3 = 0$. In this tensile test the distortion energy is then:

$$u_{dcrit} = \frac{1 + \nu}{3E} \sigma_y^2 \quad (5.12)$$

Thus, the theory predicts yielding when:

$$u_{dmax} \geq u_{dcrit} \quad (5.13)$$

$$\frac{1 + \nu}{3E} \left[\frac{(\sigma_1 - \sigma_2)^2 + (\sigma_2 - \sigma_3)^2 + (\sigma_3 - \sigma_1)^2}{2} \right] \geq \frac{1 + \nu}{3E} \sigma_y^2 \quad (5.14)$$

$$\Rightarrow \left[\frac{(\sigma_1 - \sigma_2)^2 + (\sigma_2 - \sigma_3)^2 + (\sigma_3 - \sigma_1)^2}{2} \right]^{1/2} \geq \sigma_y \quad (5.15)$$

The expression on the left can be considered an effective stress for a general stress state. We call this effective stress the *von Mises stress*: σ' . The constraint is then written more concisely as:

$$\sigma' \leq S_y \quad (5.16)$$

or with a safety factor included:

$$n = \frac{S_y}{\sigma'} \quad (5.17)$$

where

$$\sigma' = \left[\frac{(\sigma_1 - \sigma_2)^2 + (\sigma_2 - \sigma_3)^2 + (\sigma_3 - \sigma_1)^2}{2} \right]^{1/2} \quad (5.18)$$

The failure envelope (in plane stress) for the von Mises stress is shown in Fig. 5.4 as compared to the max shear stress theory. Notice that it is an ellipse that bounds the maximum shear stress envelope. In three dimensions it forms an ellipsoid. Note that it has a similar shape to MSS theory, but it results in more accurate failure predictions when compared to experimental data.

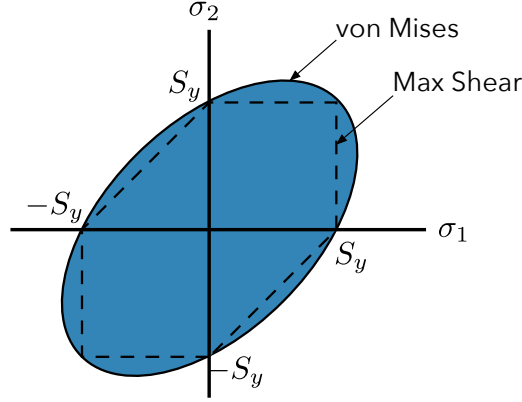


Figure 5.4: Failure envelope for distortion energy theory (von Mises) as compared to the maximum shear stress theory.

If principal stresses have not yet been computed, then an alternative formula can be used based on stresses in an arbitrary orthogonal coordinate system:

$$\sigma' = \frac{1}{\sqrt{2}} [(\sigma_x - \sigma_y)^2 + (\sigma_y - \sigma_z)^2 + (\sigma_z - \sigma_x)^2 + 6(\tau_{xy}^2 + \tau_{yz}^2 + \tau_{xz}^2)]^{1/2} \quad (5.19)$$

or more simply for a plane stress condition:

$$\sigma' = (\sigma_x^2 - \sigma_x \sigma_y + \sigma_y^2 + 3\tau_{xy}^2)^{1/2} \quad (5.20)$$

Notice that the von Mises stress allows us to reduce an arbitrary stress state with three normal stresses and three shear stresses to one representative number to predict failure. It is perhaps surprising that reducing the complexity of a stress state down to one number would be effective, but

it is and has been shown to agree very well with experimental data. This reduction is fortunate because it allows for stress state visualization of complicated geometries all through a single color map. In practice, von Mises stress is widely used and effective. The maximum shear stress theory was introduced first because it provides a simpler introduction to the concepts, but in practice it is overly conservative and not typically preferred. Generally speaking one would prefer to use the most accurate formulas available, and if additional conservatism is desired that should be built into the safety factors.

5.2.1 Yield Strength in Shear

The title of this section is a bit of a misnomer as there really isn't a quantity for yield strength in shear. However, it is a convenience that is often used and worth knowing. Consider a plane stress state that is in pure shear (no normal stresses). Using Eq. (5.20) the von Mises stress for such a state is:

$$\sigma' = \sqrt{3\tau_{xy}^2} = \sqrt{3}\tau_{xy} \quad (5.21)$$

Now we can compute the safety factor using Eq. (5.17) for this stress state:

$$n = \frac{S_y}{\sqrt{3}\tau_{xy}} \quad (5.22)$$

As a convenience let us define the quantity $S_{sy} = S_y/\sqrt{3} = 0.577S_y$ as the yield strength in shear. That allows us to write the safety factor as:

$$n = \frac{S_{sy}}{\tau_{xy}} \quad (5.23)$$

Notice how this equation parallels Eq. (5.17), but uses shear stress and $S_{sy} = 0.577S_y$ instead. We can always compute von Mises stress from the full equation and then use the normal safety factor calculation, but if only shear is involved this is a nice shortcut.

5.3 Coulomb-Mohr Theory for Ductile Materials

There is one other theory for ductile materials that is used for the less common scenario where the material is ductile, but the yield strength in compression is not equal to the yield strength in tension. The idea, proposed by Mohr, was to predict failure for three conditions: tension, compression,

and torsional shear. For each condition you would create a Mohr's circle like shown in Fig. 5.5. On the outside of these circles you could then fit a curve and use that curve as the failure envelope. In practice this method is not so straightforward because it requires three tests and the shape of the final curve is somewhat ambiguous.

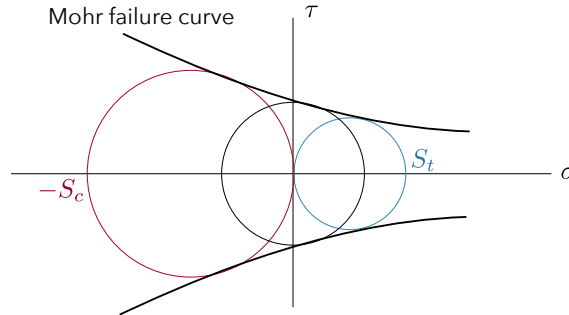


Figure 5.5: Three Mohr's circles from a tensile test, compressive test, and a torsional test. The failure curve envelopes these circles.

A variation of this theory is the *Coulomb-Mohr theory*. The idea was to simplify the bounding curve to a straight line. This has the additional benefit that a straight line can be created from just two tests: a tensile test and a compressive test. From these two pieces of information you can construct the failure envelope as seen in Fig. 5.6.

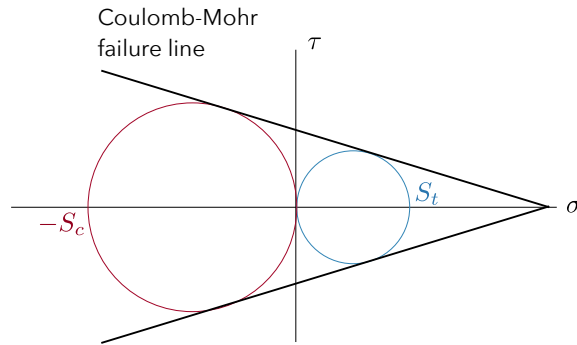


Figure 5.6: A simplified approach based on a straight line envelope around the tensile and compressive tests.

The theory predicts safety against failure as long as the corresponding

Mohr's circle remains inside this envelope. We can express this condition mathematically as :

$$\frac{\sigma_1}{\sigma_t} - \frac{\sigma_3}{\sigma_c} \leq \frac{1}{n} \quad (5.24)$$

Sometimes the ultimate strengths, rather than the yield strengths are used in this formula.

For plane stress, the failure envelope looks similar to that for maximum shear stress and is shown in Fig. 5.7. This same theory can also be used for brittle materials, which often have different strengths in tension and compression.

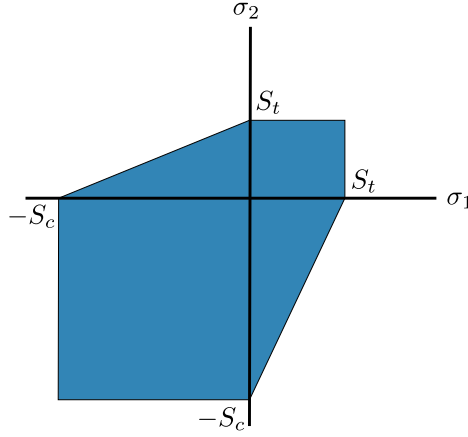


Figure 5.7: The failure envelope for Coulomb-Mohr theory under a plane stress scenario.

Chapter 6

Unsymmetric Bending

Sometimes beams have unsymmetric cross sections or have loads that do not coincide with the planes of symmetry. In these scenarios the basic bending formulas we have used will not suffice. Additional rotation of the structure will occur.

6.1 Moments of Inertia

First, we review the concepts of moments of inertia and principal axes. Consider an arbitrary cross section as shown in Fig. 6.1. There are several moments of inertia that can be computed. We have used all of these already in this book except for the products of inertia.

- The moment of inertia about the y-axis:

$$I_y = \int z^2 dA \quad (6.1)$$

- The moment of inertia about the z-axis:

$$I_z = \int y^2 dA \quad (6.2)$$

- The yz product of inertia:

$$I_{yz} = \int yz dA \quad (6.3)$$

- The polar moment of inertia about point o :

$$J_o = \int r^2 dA = I_y + I_z \quad (6.4)$$

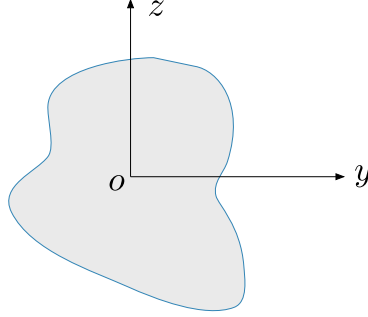


Figure 6.1: An arbitrary cross section.

The *parallel axis theorem* allows us to transfer moments of inertia from the centroid of a cross section to any other arbitrary location. Using the notation shown in Fig. 6.2 we can make the following transformation:

$$I_y = I_{y_c} + A\Delta z^2 \quad (6.5)$$

$$I_z = I_{z_c} + A\Delta y^2 \quad (6.6)$$

$$I_{yz} = I_{yz_c} + A\Delta y\Delta z \quad (6.7)$$

$$J_o = J_c + A\Delta r^2 \quad (6.8)$$

where A is the cross sectional area.

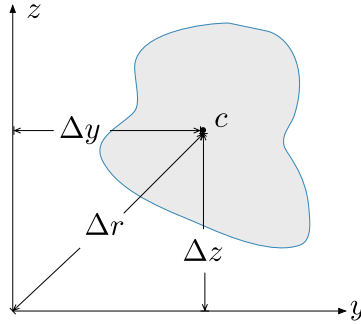


Figure 6.2: Offsets used in the parallel axis theorem.

The sign is important for the offsets in the product of inertia case (in the other moments of inertia the offset is squared so the sign is irrelevant). It does not matter whether your offsets go from the centroid to the new point of interest or the other way around, as long as you use the same procedure

for both offsets. Note that if the cross section has an axis of symmetry then the corresponding products of inertia will be zero (which is why we didn't deal with products of inertia earlier).

For a given point o , there is some orientation for the coordinate system about which the moments of inertia are at a maximum and a minimum. These are called the *principal axes*, and the corresponding moments of inertia are called the *principal moments of inertia*. Just like how principal stresses occur in axes where the shear stress is zero, principal moments occur where the products of inertia are zero. The counterclockwise angle at which the principal axes is located relative to the current axes is:

$$\tan(2\theta) = \frac{2I_{yz}}{I_z - I_y} \quad (6.9)$$

and the principal moments of inertia are:

$$I_{max,min} = \frac{I_y + I_z}{2} \pm \sqrt{\left(\frac{I_y - I_z}{2}\right)^2 + I_{yz}^2} \quad (6.10)$$

In three-dimensions, we solve for the principal moments of inertia in the same way as we solve for principal stresses for a general 3-D stress state. Namely, by using an eigenanalysis:

$$I_m = \begin{bmatrix} I_{xx} & I_{xy} & I_{xz} \\ I_{xy} & I_{yy} & I_{yz} \\ I_{xz} & I_{yz} & I_{zz} \end{bmatrix} \quad (6.11)$$

$$|I_m - \lambda I| = 0 \quad (6.12)$$

where I is the identity matrix.

6.2 Unsymmetric Bending of Straight Beams

Unsymmetric bending occurs if a beam does not have a plane of symmetry (i.e., the product of inertia is nonzero), or if the loads are not aligned with that plane of symmetry (e.g., bidirectional bending). When unsymmetric bending occurs the cross section will rotate about a neutral axis that is not necessarily parallel to the moment. As alluded to, bidirectional bending, which we have already been introduced to, is usually a case where unsymmetric bending occurs although we did not mention this previously.

Figure 6.3 shows an example of a bending moment applied to an unsymmetric cross section. Note that the neutral axis does not align either

with a plane of symmetry for the cross section or with the direction of the applied moment. The derivation of the equations for unsymmetric bending are provided in Appendix B. The result is that the axial stress is given by:

$$\sigma_x = \frac{(-M_y I_{yz} - M_z I_y)y + (M_y I_z + M_z I_{yz})z}{I_y I_z - I_{yz}^2} \quad (6.13)$$

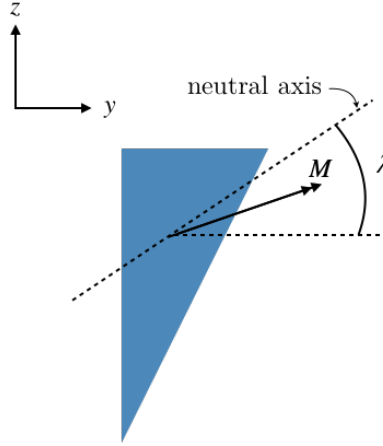


Figure 6.3: A unsymmetric cross section with an applied bending moment. The neutral axis is also shown. The $+x$ direction is out of the page.

In this equation x is the axial direction, and *assumes the cut face points in the $+x$ direction*. The other coordinates y and z can be of any orientation, but the origin of the coordinate system must be located at the cross section's centroid. This means that moments of inertia *must be computed about the cross section's centroid*.

We can find the neutral axis by realizing that it is the line of points for which $\sigma_x = 0$. If we define the angle of the neutral axis as λ then from the geometry we can say that:

$$\tan \lambda = \frac{z}{y} \quad (6.14)$$

Solving the above equation for z/y (when $\sigma_x = 0$) gives the following formula for the angle to the neutral axis:

$$\tan \lambda = \frac{M_y I_{yz} + M_z I_y}{M_y I_z + M_z I_{yz}} \quad (6.15)$$

A positive angle λ corresponds to a counter-clockwise rotation from the $+y$ axis.

If y and z happen to be principal axes then $I_{yz} = 0$ and the flexural stress formula reduces to the basic biaxial bending equation that we have seen before:

$$\sigma_x = -\frac{M_z y}{I_z} + \frac{M_y z}{I_y} \quad (6.16)$$

If the geometry makes finding principal axes obvious, then it is desirable to choose a coordinate system aligned with those symmetry axes in order to simplify the stress analysis. But, if the principal axes are not obvious, then it is easier to just use the full unsymmetric bending equation. You could first compute the principal axes, then recompute all the properties in the new axes in order to use the shorter biaxial bending equation, but that's a wasted effort. By the time you've computed the moments and products of inertia in order to find the principal axis, you already have all you need to use the unsymmetric bending equation directly.

Also note that principal axes and neutral axis are not the same. This is most easily seen by considering a simple section like a rectangle with bidirectional bending. We've studied several problems like this already and have shown that the maximum stress is at one of the corners. We didn't discuss what the neutral axis was for these cases, but if you think about it you should be able to convince yourself that it must be at an angle with respect to the rectangle.

You could calculate its orientation precisely by using Eq. (B.12) with $I_{xy} = 0$:

$$\tan \lambda = \frac{M_z I_y}{M_y I_z} \quad (6.17)$$

As a simple example consider a rectangular cross section aligned with the axes and with $I_y = 2I_z$. Let's also assume that the applied moments are as follows: $M_y = 2M_z$. Then the above formula gives $\lambda = 45^\circ$. Thus, for this example the principal axes are at 0 and 90 degrees, but the neutral axis is at 45 degrees.

To restate: the neutral axis is very different from the principal axes. The principal axes are purely a function of the geometry—for the rectangle those axes go straight through the sides. The neutral axis depends on the geometry *and* the loading. As we change the loads on a rectangular cross-section with bidirectional bending, the angle of the neutral axis changes also.

Chapter 7

Buckling

Buckling is an important failure mode to design for, particularly because it is difficult to predict, sudden, and usually catastrophic. Standing on an aluminum can is a common party trick. If there are no imperfections in the can, and you stand on it just right, it will hold your weight. Even though the can has very thin sidewalls, the stress is well below the yield strength of aluminum so there is no static failure. However, a slight deformation or imbalance will cause the can to buckle leading to a sudden collapse. To repeat: analyzing for static failure alone is insufficient. Buckling is an critical design criteria for many engineering machines including aircraft wings, buildings, bridges, etc.

7.1 Euler Column Buckling

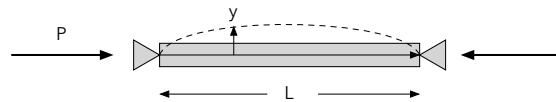


Figure 7.1: A pinned-pinned column with a compressive load.

Consider a column pinned at both ends under a compressive load (Fig. 7.1). As the load increases, the column will deform as shown in the dashed line. Keep in mind that *buckling only occurs for compressive loads*. For a beam in bending we can show that the moment is related to the curvature of the beam with the following relationship (see Eq. (2.10) where the curvature κ

is given by the second derivative d^2y/dx^2):

$$M(x) = EI \frac{d^2y}{dx^2} \quad (7.1)$$

For this particular case, a column under compressive load, the moment is just $M(x) = -Py(x)$. This gives:

$$-Py = EI \frac{d^2y}{dx^2} \quad (7.2)$$

We can rearrange this into a differential equation of the form:

$$\frac{d^2y}{dx^2} + \omega^2 y = 0 \quad (7.3)$$

where

$$\omega = \sqrt{\frac{P}{EI}} \quad (7.4)$$

This ordinary differentiation equation (ODE) should look familiar. It is the same form as a mass on a spring ($\ddot{x} + \omega x = 0$, where $\omega = \sqrt{k/m}$). The general solution to this ODE is:

$$y = A \cos(\omega x) + B \sin(\omega x) \quad (7.5)$$

where A and B are unknown constants that are determined from the boundary conditions. For a pinned-pinned column the boundary conditions are $y(0) = 0$ and $y(L) = 0$. The first boundary condition yields:

$$A = 0 \quad (7.6)$$

while the second boundary condition yields:

$$0 = B \sin(\omega L) \quad (7.7)$$

This gives either the trivial solution $B = 0$ (which is not helpful), or $\omega L = n\pi$ for $n = 1, 2, 3, \dots$. Substituting in the definition of ω gives:

$$\begin{aligned} \sqrt{\frac{P}{EI}} L &= n\pi \\ P &= \frac{n^2 \pi^2 EI}{L^2} \end{aligned} \quad (7.8)$$

This equation says that there are multiple critical loads, and each corresponds to different mode shapes. This first one corresponds to:

$$y = B \sin\left(\frac{n\pi x}{L}\right), \quad (7.9)$$

which gives the dashed line shape we saw in Fig. 7.1. For failure due to buckling only the first buckling load matters, so the critical (or minimum) buckling load is:

$$P_{cr} = \frac{\pi^2 EI}{L^2} \quad (7.10)$$

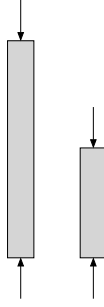


Figure 7.2: A beam that is half as long has four times the buckling strength.

This is Euler's formula for buckling. Note the primary dependence on length. By halving the length of a column (Fig. 7.2) the critical load increases by a factor of 4. In other words the buckling load of a bar can be increased significantly by decreasing the length between supports. This technique is commonly used to increase buckling strength. For example, in an aircraft ribs will be added to decrease the buckling length between the spar (Fig. 7.3) or more importantly between thinner members that run parallel to the spar called stringers. Note also that using a stronger material (e.g., increasing S_y) will have zero impact on the critical buckling load. The material is not completely irrelevant as the stiffness (E) appears in the equation, but this effect is relatively minor.

We can generalize this formula for other boundary conditions by writing it in the form:

$$P_{cr} = \frac{C\pi^2 EI}{L^2} \quad (7.11)$$

where C is a constant that depends on the boundary condition ($C = 1$ for the pinned-pinned case we just examined). To derive the others scenarios we

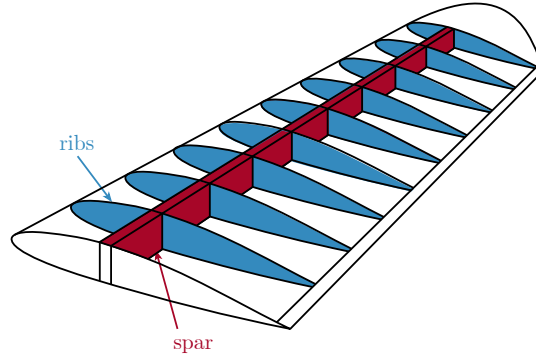


Figure 7.3: Simplified representation of aircraft wing structure. Figure adapted from [this figure](#) and [this figure](#), both by MLWatts, Wikimedia Commons, public domain.

actually need to use a more general formula for bending. This approach leads to a fourth order ODE, but is otherwise the same process. This second order ODE corresponds only to this boundary condition, and was used to simplify the discussion. The results for other boundary conditions are summarized in Table 7.1. Note that these boundary conditions are theoretical and in practice more conservative values are usually used for fixed-pinned and fixed-fixed (often around $C = 1.2$).

Table 7.1: Different boundary conditions for a column with corresponding coefficients used in Euler's formula.

boundary condition	C
fixed-free	$1/4$
pinned-pinned	1
fixed-pinned	≈ 2
fixed-fixed	4

We can see that if we fix one of the sides of the column that was pinned, then the critical buckling load increases. However, a perfectly fixed boundary condition is hard to achieve in real life, so often a more conservative value ($C = 1$) is used for fixed-pinned, and fixed-fixed. We can rearrange

the buckling equation by writing it in the form of a stress:

$$\begin{aligned} P_{cr} &= \frac{C\pi^2 EI}{L^2} \\ \frac{P_{cr}}{A} &= \frac{C\pi^2 EI}{AL^2} \end{aligned} \quad (7.12)$$

where the left hand side has units of stress. For convenience we define the radius of gyration as $k = \sqrt{I/A}$ in order to group the geometric terms for the cross section. The result is:

$$\boxed{\frac{P_{cr}}{A} = \frac{C\pi^2 E}{(L/k)^2}} \quad (7.13)$$

where L/k is called the slenderness ratio.

We can plot the variation in P_{cr}/A as a function of the slenderness ratio as seen by the blue curve in Fig. 7.4. Recall that P_{cr}/A is not a measure of material strength, but of buckling strength. In other words even if you use a stronger material the buckling strength would not change at all (for a fixed E). However, we know we can't just keep increasing the load that can be carried. At some point on the graph the yield stress will be reached. This is what the red line represents in Fig. 7.4.

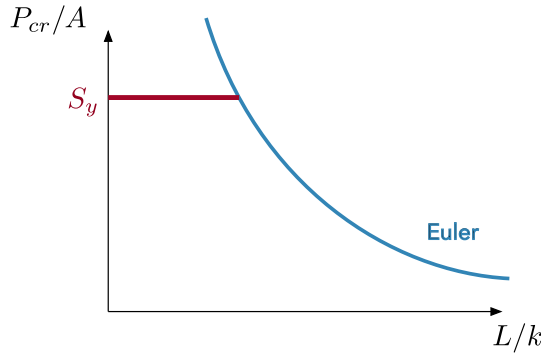


Figure 7.4: Buckling strength from Euler's formula with a cap from the yield strength.

7.2 Johnson Buckling

Ideally, this would be the end of the story, but experimental tests show that buckling loads do not follow the blue Euler curve all the way up to the yield point. Euler theory only works up to a point, and this point is generally taken to be where $P_{cr}/A = S_y/2$. This corresponds to a cut-off point of:

$$\left(\frac{L}{k}\right)_{cr} = \left(\frac{2\pi^2 CE}{S_y}\right)^{1/2} \quad (7.14)$$

For slenderness ratios smaller than this cut-off point, a different theory is used, known as Johnson's theory. This theory just fits a quadratic function between the two end points as shown in Fig. 7.5. In equation form, Johnson's theory is:

$$\frac{P_{cr}}{A} = S_y - \left(\frac{S_y L}{2\pi k}\right)^2 \frac{1}{CE} \quad \text{for } \frac{L}{k} \leq \left(\frac{L}{k}\right)_{cr} \quad (7.15)$$

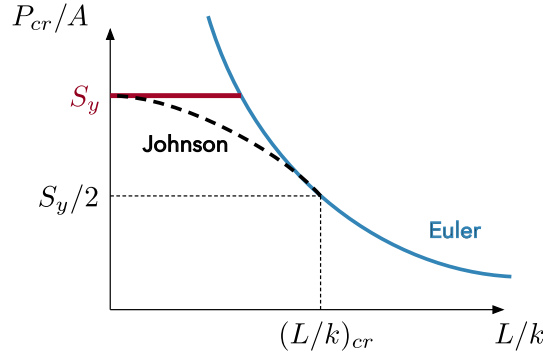


Figure 7.5: Johnson's formula bridges between Euler's formula and the yield strength.

To summarize, if the slenderness ratio is high (above the critical value) we use Euler's formula. If the slenderness ratio is low (below the critical value) we use Johnson's formula. In equation form:

$$\frac{P_{cr}}{A} = \begin{cases} \frac{C\pi^2 E}{(L/k)^2} & \text{if } L/k > (L/k)_{cr} \\ S_y - \left(\frac{S_y L}{2\pi k}\right)^2 \frac{1}{CE} & \text{if } L/k < (L/k)_{cr} \end{cases} \quad (7.16)$$

One should also keep in mind, that checking buckling does not remove the need to check for static failure. It is possible to be safe from buckling but fail under static loading or vice-versa.

Chapter 8

Reliability

Failure predictions cannot assume deterministic behavior. Material properties, loads, and geometry all have inherent variability. One way to address this uncertainty is with safety factors. Safety factors are easy to apply but are fairly crude. An alternative approach is to use statistics to predict the probability that the structure will not fail, which is also known as its *reliability*.

8.1 Brief Statistics Review

This section provides a brief overview of some principles from statistics. It is not a comprehensive review as it is expected that you have been introduced to these concepts previously.

8.1.1 Random Variables

A random variable is an outcome or measurement with some uncertainty associated with its value. Consider a batch of 100 tensile-test specimens; you would expect differences in the yield strength amongst the specimens. The yield strength of the material is a random variable. We can tabulate all the different outcomes of our random variable into a probability density function (PDF). We usually denote the probability distribution function with a lowercase f .

If x is a continuous variable the PDF must have the property that

$$\int_{-\infty}^{\infty} f(x)dx = 1 \quad (8.1)$$

Similarly, we can find the probability of an event occurring in a given interval from the equation

$$P[a \leq X \leq b] = \int_a^b f(x)dx \quad (8.2)$$

A related function is the cumulative density function (CDF). By convention we usually denote the CDF with a capital F . The CDF describes the probability that an event will have a value less than or equal to x . In other words

$$F(x) = \int_{-\infty}^x f(x)dx \quad (8.3)$$

From the definition we can see that curve will always approach 1. By differentiating we can derive the following relationship between the CDF and the PDF:

$$\frac{dF(x)}{dx} = f(x) \quad (8.4)$$

Figure 8.1 shows an example PDF and its corresponding CDF.

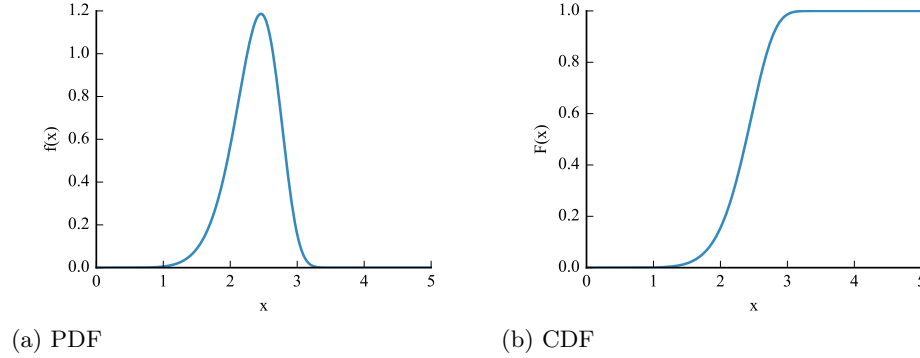


Figure 8.1: An example probability density function (PDF) and its corresponding cumulative density function (CDF).

8.1.2 Expectation and Variance

The expectation is also called the mean or average. It is defined as:

$$E(X) = \mu_x = \int_{-\infty}^{\infty} x f(x) \quad (8.5)$$

where $f(x)$ is the PDF. For discrete measurements it is defined as:

$$E(X) = \mu_x = \sum_{i=1}^N x_i f(x_i) \quad (8.6)$$

Some important properties of expectation are:

$$\begin{aligned} E(X + Y) &= E(X) + E(Y) \\ E(aX) &= aE(X) \text{ where } a \text{ is a constant} \end{aligned} \quad (8.7)$$

To estimate the expected value for a sample, we use the sample mean (we will not distinguish between population statistics and sample statistics in notation or usage):

$$\mu_x = \frac{1}{N} \sum_{i=1}^N x_i \quad (8.8)$$

Variance is a measure of spread. The deviation of a given sample is $(x_i - \mu_x)$. The sum of all of these deviations is always zero (that is the definition of a mean), so instead we sum the square of the deviations:

$$Var(X) = E[(X - \mu)^2] = \sigma^2 = \int_{-\infty}^{\infty} (x - \mu)^2 f(x) dx = \int_{-\infty}^{\infty} x^2 f(x) dx - \mu^2 \quad (8.9)$$

The unbiased estimate sample variance is (note the $N - 1$):

$$\begin{aligned} \sigma_x^2 &= \frac{1}{N-1} \sum_{i=1}^N (x_i - \bar{x})^2 \\ &= \frac{1}{N-1} \left(\sum_{i=1}^N x_i^2 - N\bar{x}^2 \right) \end{aligned} \quad (8.10)$$

The standard deviation (σ) is simply the square root of the variance (σ^2).

8.1.3 Common Probability Distribution

One of the most familiar probability distributions is the Gaussian or normal distribution:

$$f(x) = \frac{1}{\sigma\sqrt{2\pi}} \exp \left[-\frac{1}{2} \left(\frac{x - \mu}{\sigma} \right)^2 \right] \quad (8.11)$$

The normal distribution is used so commonly that we normalize the deviation and tabulate values for corresponding probabilities in what is called a standard normal table. The normalization used is

$$z = \frac{x - \mu}{\sigma} \quad (8.12)$$

The normal distribution as a function of z is shown in Fig. 8.2. Appendix C tabulates quantities for a standard normal distribution. Values not on the table can be found from interpolation. Alternatively, most calculators and programming languages provide direct calculations for a standard normal distribution.

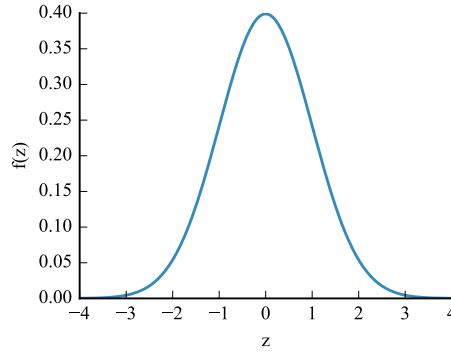


Figure 8.2: A normal or Gaussian distribution.

Various other distributions exist like the uniform, lognormal, and Weibull distributions. The lognormal and Weibull distribution are asymmetric and only have positive values.

8.1.4 Forward Propagation

Consider a calculation for torsional shear stress in a beam:

$$\tau = \frac{Tr}{J} \quad (8.13)$$

If we know the variability of inputs T and J , for example, what is the variability of the output τ ? *Forward propagation* methods allow us to estimate output variabilities from known input variabilities. There are a number of forward propagation methods, but in this text we will only study one: first-order perturbation. This method assumes independent inputs and that the PDF of every input is symmetric. We will generally assume Gaussian inputs, which satisfy the symmetry condition.

Given some output function f that depends on inputs x_i , the statistics of the output are given as follows:

$$\mu_f = f(\mu_x) \quad (8.14)$$

$$\sigma_f^2 = \sum_{i=1}^N \left(\frac{\partial f}{\partial x_i} \sigma_{x_i} \right)^2 \quad (8.15)$$

where all partial derivatives are evaluated using mean quantities.

So for our simple example above we could estimate the mean of the shear stress as (assuming r was deterministic):

$$\mu_\tau = \frac{Tr}{J} \quad (8.16)$$

where mean values are used for T and J . The variance of the shear stress is estimated as:

$$\begin{aligned} \sigma_\tau^2 &= \left(\frac{\partial \tau}{\partial T} \sigma_T \right)^2 + \left(\frac{\partial \tau}{\partial J} \sigma_J \right)^2 \\ &= \left(\frac{r}{J} \sigma_T \right)^2 + \left(\frac{-Tr}{J^2} \sigma_J \right)^2 \end{aligned} \quad (8.17)$$

where again mean values are used for T and J .

8.2 Reliability

We can now put statistics to use to predict reliability. Previously, when examining failure criteria, we used a safety factor defined as:

$$\text{Safety Factor} = \frac{\text{Strength}}{\text{Load}} \quad (8.18)$$

Reliability is defined as the probability that the strength exceeds the load:

$$R = \text{prob}(\text{Strength} > \text{Load}) \quad (8.19)$$

Consider the probability distribution for the strength and the probability distribution for the load as depicted in Fig. 8.3. From the figure we see although most of the time the strength will exceed the load, there is still a significant probability that failure could occur. We want to quantify what that probability is.

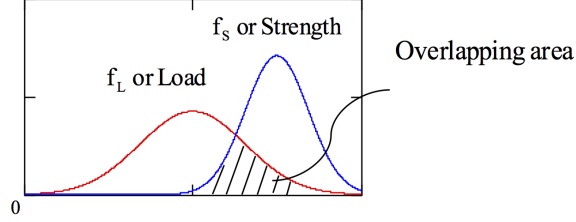


Figure 8.3: Depiction of separate probability distributions for strength and for a load.

Let's define a new variable x which is the strength S minus the load L : $x = S - L$. Then the reliability is:

$$R = \text{prob}(x > 0) \quad (8.20)$$

We can find the mean and standard deviation of x using the forward propagation method we learned in the last section. The mean is given by:

$$\mu_x = \mu_S - \mu_L \quad (8.21)$$

The variance is:

$$\sigma_x = \sqrt{\left(\frac{\partial x}{\partial S} \sigma_S\right)^2 + \left(\frac{\partial x}{\partial L} \sigma_L\right)^2} \quad (8.22)$$

$$= \sqrt{\sigma_S^2 + \sigma_L^2} \quad (8.23)$$

The distribution for x is depicted in Fig. 8.4. In general, this distribution need not be normal. However, if S and L are both normally distributed then x is also normally distributed. In this text we will assume normally distributed inputs.

In order to use a standard normal function or table, we need to compute the corresponding z-score. In words, the z-score tells us how many standard deviations are we are away from the mean. Recall that:

$$z = \frac{x - \mu}{\sigma} \quad (8.24)$$

In our case, we are interested in the case corresponding to $x = 0$ so we can determine $\text{prob}(x > 0)$. The z-score for our case where $x = 0$ is:

$$z^* = -\frac{\mu_x}{\sigma_x} \quad (8.25)$$

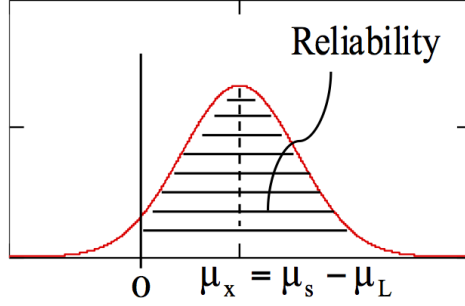


Figure 8.4: Probability distribution for the reliability.

Thus our criteria $prob(x > 0)$ corresponds to $prob(z > z^*)$. This situation is also depicted in Fig. 8.4. From a standard normal function/table (like the one in Appendix C) we can lookup a value for the CDF. Let's call that value p :

$$p = CDF(z^*) \quad (8.26)$$

Recall that the CDF gives us the area under the curve below that z^* value and we want $p(z > z^*)$, which is given by:

$$R = 1 - p \quad (8.27)$$

Let's consider a simple example. Assume that

$$S \sim \mathcal{N}(250, 7.07) \text{ MPa} \quad (8.28)$$

$$L \sim \mathcal{N}(220, 10) \text{ MPa} \quad (8.29)$$

This is a standard notation that means that the strength is normally distributed with a mean of 250 MPa and a standard deviation of 7.07 MPa, with a corresponding interpretation for the load distribution (see Fig. 8.5).

Following our procedure where we define $x = S - L$, we can compute the mean and standard deviation of x as:

$$\mu_x = \mu_S - \mu_L = 30 \text{ MPa} \quad (8.30)$$

$$\sigma_x = \sqrt{\sigma_S^2 + \sigma_L^2} = 12.25 \text{ MPa} \quad (8.31)$$

The z-score corresponding to $x = 0$, which defines failure, is:

$$z^* = \frac{0 - \mu_x}{\sigma_x} = -2.45 \quad (8.32)$$

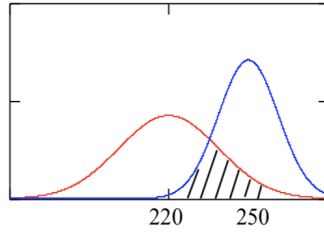


Figure 8.5: The strength distribution (in blue) and the load distribution (in red) for this example problem.

We now want to find the reliability, which is $\text{prob}(x > 0)$ or $\text{prob}(z > -2.45)$.

Using Appendix C we see that $z = 2.45$ corresponds to a CDF (area to the left) of 0.992857. However, we want the area to the right of $z = -2.45$. From the symmetry of the normal distribution these two values are equivalent (compare for example Fig. C.1 and Fig. 8.6). Thus the reliability is 99.29%, or the failure of probability is 0.71%. While this problem determined reliability for given conditions, more often we perform the inverse. Namely, we specify a desired reliability level and solve backwards to determine, for example, the requisite geometry sizing.

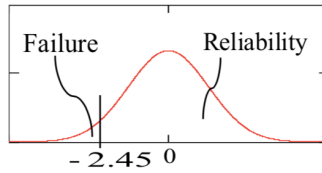


Figure 8.6: The reliability is the area under the normal distribution to the right of our z value.

Chapter 9

Fatigue

This chapter does not provide a thorough description of fatigue. Instead, we will defer to Shigley for a description of fatigue analysis. The purpose of this chapter is help you navigate the process and be aware of some of the nuances that are easy to overlook.

9.1 Process

There are four scenarios we have discussed for analyzing fatigue:

- Fully reversed simple loading (i.e., mean zero)
- Fluctuating simple loading
- Combined simple loading
- Complex loading

Only the first three scenarios are emphasized in this course. The analysis steps for all cases are the same:

1. Gather material data
2. Estimate (or gather) endurance limit
3. Compute stress concentration factors (if applicable)
4. Compute stresses and apply stress concentration factors
5. Check for infinite life

6. If not infinite life, compute number of cycles for finite life (or safety factor for a given number of cycles)
7. Check for yielding

9.2 Case 1: Fully Reversed Simple Loading

1. **Gather material data.** The relevant material data includes the ultimate strength S_{ut} , the yield strength S_y , and if available from test data the unmodified endurance limit S'_e . If the latter is not available from test data, and you are using steel, you can use the formula from (6-8) in Shigley.
2. **Compute the endurance limit** by applying all the Marin factors.

$$S_e = k_a k_b k_c k_d k_e k_f S'_e \quad (9.1)$$

3. **Compute the fatigue stress-concentration factors** (if necessary). First find the static stress concentration factors from Table A-15 (K_t or K_{ts}). Then obtain the notch sensitivity, either from the charts or the equations (Figs. 6-20 and 6-21, Eqns. 6-34 and 6-35). The notch sensitivity just defines a ratio between the static stress concentration factors and the fatigue stress concentration factors. The notch sensitivity is a function of the material and geometry. You can compute the fatigue stress concentration factor K_f as

$$K_f = 1 + q(K_t - 1) \quad (9.2)$$

and similarly for K_{fs} (for shear stresses):

$$K_{fs} = 1 + q_s(K_{ts} - 1) \quad (9.3)$$

4. **Compute the magnitude of the stress reversal and apply the stress concentration factors.**

$$\sigma_{rev} = K_f \sigma_0 \quad (9.4)$$

5. **Check for infinite life** (i.e., is $\sigma_{rev} \leq S_e$).
6. **If not infinite life, determine the corresponding number of cycles for a given safety factor**, or determine the safety factor for

a given number of cycles. First, the constants for the finite-life region are needed (a and b in $S_f = aS_{ut}^b$). These could be determined from experimental data using linear regression in log-log space. Or, in this class, we can use the simplified formulas in the book that fit between two points (Eq. 6-14, 6-15, and Fig 6-18): The safety factor in fatigue can be computed as

$$n_f = \frac{S_f}{\sigma_{rev}} \quad (9.5)$$

where

$$S_f = aN^b \quad (9.6)$$

Or, the number of cycles to failure can be computed as

$$N = \left(\frac{n_f \sigma_{rev}}{a} \right)^{1/b} \quad (9.7)$$

7. **Check for yielding.** This is a straightforward check:

$$n_y = \frac{S_y}{\sigma_{rev}} \quad (9.8)$$

9.3 Case 2: Fluctuating Simple Loading

1. **Material Data.** Same as Case 1
2. **Endurance Limit.** Same as Case 1
3. **Stress Concentrations.** Same as Case 1
4. **Stress Magnitude.** Since the load is not fully reversed both the midrange and alternating stresses need to be computed. Stress concentration factors should be applied to both.

$$\sigma_{m0} = \frac{\sigma_{max} + \sigma_{min}}{2} \quad (9.9)$$

$$\sigma_{a0} = \frac{|\sigma_{max} - \sigma_{min}|}{2} \quad (9.10)$$

$$\sigma_m = K_f \sigma_{m0} \quad (9.11)$$

$$\sigma_a = K_f \sigma_{a0} \quad (9.12)$$

5. **Infinite Life.** With a nonzero mean we need a different approach, and in class we use Goodman's theory. If $\sigma_m \geq 0$

$$\frac{\sigma_a}{S_e} + \frac{\sigma_m}{S_{ut}} = \frac{1}{n_f} \quad (9.13)$$

else if $\sigma_m < 0$

$$n_f = \frac{S_e}{\sigma_a} \quad (9.14)$$

If you have pure torsion (shear stress), then you must use a reduced ultimate strength as described in Section 6-13 of Shigley. $S_{su} = 0.67S_{ut}$. Use this reduced S_{su} in replace of S_{ut} only in Eq. (9.13) above.

6. **Finite Life.** If n_f is less than one, then there is a finite life and you need to determine the finite life number of cycles or factor of safety just as done in Item 6. To use those equations you need to convert the midrange and alternating stresses into an equivalent fully reversed stress. As discussed in class, this is done for Goodman's theory using:

$$\sigma_{rev} = \frac{\sigma_a}{1 - \frac{\sigma_m}{S_{ut}}} \quad (9.15)$$

If you have pure torsion (shear stress), then you must use a reduced ultimate strength as described in Section 6-13 of Shigley. $S_{su} = 0.67S_{ut}$. Use this reduced S_{su} in replace of S_{ut} only in Eq. (9.15) above.

7. **Yielding.** This is still straightforward.

$$n_y = \frac{S_y}{\sigma_m + \sigma_a} \quad (9.16)$$

If you have pure torsion (shear stress), you need to compare to the "shear yield strength" which is $S_{sy} = 0.577S_y$ (or equivalently convert the shear stress to a von Mises stress before comparing to the yield stress).

9.4 Case 3: Combined Simple Loading

1. **Material Data.** Same as Case 1
2. **Endurance Limit.** Same as Case 1, except do not apply k_c (loading factor) to the endurance limit because there are multiple loads. This correction is embedded in step 4.

3. **Stress Concentrations.** Same as Case 1.
4. **Stress Magnitudes..** Similar to Case 2, except that a von Mises calculation is needed for the midrange and alternating stress components separately. The equation is slightly complicated because the fatigue stress concentration factors differ for bending, axial loading, and torsion so be sure to apply each factor to the corresponding stress. The axial correction factor of 0.85, only applies to the alternating component (because we are placing it here instead of with the endurance limit). The bending correction factor is 1.0, and the Marin factor for torsional should not be used because it is already accounted for in the von Mises stress calculation. Split σ into σ_m and σ_a , similarly split τ into τ_m and τ_a . Then combine them into von Mises stresses for the mean and alternating stresses separately.

mean:

$$\begin{aligned}\sigma_m &= K_{fbending}\sigma_{m-bending} + K_{faxial}\sigma_{m-axial} \\ \tau_m &= K_{ftorsion}\tau_{m-torsion} \\ \sigma'_m &= \sqrt{\sigma_m^2 + 3\tau_m^2}\end{aligned}\tag{9.17}$$

alternating:

$$\begin{aligned}\sigma_a &= K_{fbending}\sigma_{a-bending} + K_{faxial}\frac{\sigma_{a-axial}}{0.85} \\ \tau_a &= K_{ftorsion}\tau_{a-torsion} \\ \sigma'_a &= \sqrt{\sigma_a^2 + 3\tau_a^2}\end{aligned}\tag{9.18}$$

5. **Infinite Life.** Same as Case 2
6. **Finite Life.** Same as Case 2
7. **Yielding.** You can use the same approach as in Case 2, except use the von Mises stresses from step 4.

$$n_y = \frac{S_y}{\sigma'_m + \sigma'_a}\tag{9.19}$$

This is conservative. More accurately yielding should be checked by first combining the mean and alternate stresses into σ_{max} and τ_{max} and then computing the corresponding maximum von Mises stress. However, because the simpler check is always conservative, and because we are computing those values anyway, it is easier just to use this check.

If our safety factor is larger than 1, then we are safe. However, if it is less than 1, we may or may not be yielding and so need to check using the more accurate approach. There is no need to use the more accurate check if the simple solution already shows we are safe from yielding.

Chapter 10

Fatigue 2

Up to this point we have only examined static loads. Many structures are subject to time-varying loads. These dynamic loads, and the failure caused by dynamic loads (fatigue), are the subject of this chapter.

10.1 Introduction

This video contains a good overview of the concept of fatigue: https://youtu.be/LhUclxBUV_E. Perhaps the most familiar example of fatigue is a paperclip. We can bend a paperclip once and it does not fail, but if we repeated bend and unbend the paperclip it fractures. Why is that? The study of fatigue is complex, but at a basic level is governed by crack propagation. Even though the loads on the material may be well below their yield strength, microscopic cracks begin to form and repeated tensile loading causes these cracks to grow and propagate. Eventually the cracks will grow large enough that the structure fractures.

Fatigue, like buckling, is particularly dangerous as it is difficult to predict, usually catastrophic, and may occur suddenly. Because of the difficulty in mathematical prediction models, most fatigue analyses are based on empirical methods. In this text we use what is called a stress-life approach. This type of approach is primarily only appropriate for high cycle fatigue (structures that are designed to withstand more than a thousand load cycles). It is not the most accurate approach, but is relatively easy to use and widely familiar.

At the heart of a basic fatigue analysis is the S - N diagram. This diagram was seen in the video for a fully reversed axial load and a typical diagram is plotted in Fig. 10.1 on a log-log scale. The y axis contains various stress

magnitudes for a fully reversed load. The x contains the corresponding number of cycles before fatigue failure. We plot on a log scale for two reasons: the number of cycles can vary across many orders of magnitude, and on a log-log scale the relationships are often well approximated with linear segments.

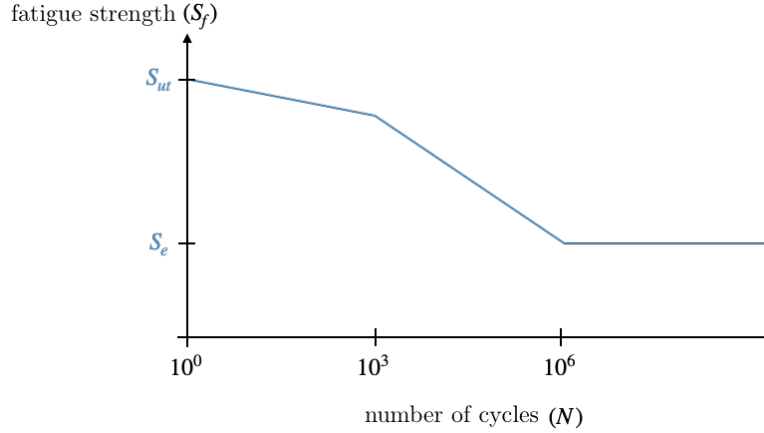


Figure 10.1: A typical S-N diagram for a material with an endurance limit plotted on a log-log scale. The values for the number of cycles are not fundamental, just representative.

If there was only one cycle ($N = 10^0$) then the corresponding load that would cause a fracture is the ultimate strength. As the magnitude of the cyclic load is reduced, the structure can be expected to carry that reduced load for more load cycles (hence the negative slope). There may be more than one linear region. In the example plot the leftmost line segment corresponds to low-cycle fatigue (not of interest in our method), and the next linear segment to high cycle fatigue. In other cases one line represents both low and high cycle fatigue.

For some materials, most notably steel, the S - N diagram plateaus as shown in the figure (shown at a million cycles in this example, but that number varies). This stress level is called the *endurance limit* (S_e) and will be discussed in more detail in a subsequent section. The significance of this plateau is that if the magnitude of the cyclic load is below the endurance limit then that level of stress could be maintained indefinitely. Such a structure is said to have *infinite life*. If the structure has a higher level of stress then it has a *finite life* corresponding to some number of cycles. For design purposes we need to consider how long the structure is intended to last, and

thus how many cycles it must withstand.

It should be stressed that the methods of this chapter are highly approximate and are only meant for early stage design. The S - N diagram is actually not a sharp curve as shown in Fig. 10.1, but is rather a wide band of values.

10.2 Endurance Limit

As introduced in the previous section, for some materials the S - N diagram plateaus at what is called the endurance limit. Other materials, like aluminum, do not have an endurance limit. In this text we will focus on steel, which does have an endurance limit. The purpose of this section is to estimate that value. Ideally, it should be estimated from experimental measurements using the material, geometry, and loading conditions of the actual structure. However, for early-stage design it is desirable to have a simple approach to estimate the endurance limit.

The first step is to compute an *unmodified endurance limit* (S'_e). An unmodified endurance limit depends only on material properties and not on the geometry, loading, or other operating conditions. Because it depends only on material we may be able to more universally estimate it. Based on various experimental studies [ref], a rough approximation of the unmodified endurance limit for steel is:

$$S'_e = \begin{cases} 0.5 S_{ut} & \text{for } S_{ut} \leq 200 \text{ kpsi (1400 MPa)} \\ 100 \text{ kpsi (700 MPa)} & \text{for } S_{ut} > 200 \text{ kpsi (1400 MPa)} \end{cases} \quad (10.1)$$

where S_{ut} is the ultimate strength.

We then correct the unmodified endurance limit by multiple factors in order to get the final endurance limit:

$$S_e = k_{surf} k_{size} k_{load} k_{temp} k_{reli} S'_e \quad (10.2)$$

The corrections provide modification based on the surface finish, component size, loading type, environment temperature, and desired reliability respectively. Each of these corrections, which are also known as Marin factors, are discussed in the following subsections.

10.2.1 Surface Finish

An ideal surface is highly smooth and polished, and such surfaces are used in obtaining unmodified endurance limits. However, real structures have

a variety of surface imperfections, which are more likely to facilitate crack initiation and propagation. Noll and Lipson [ref] compiled experimental data that can be used to estimate the surface finish Marin factor as follows:

$$k_{surf} = \alpha S_{ut}^{\beta} \quad (10.3)$$

where α and β come from Table 10.1. This procedure can sometimes produce values of k_{surf} that exceed one, but that should not be allowed. In other words you should modify k_{surf} as:

$$k_{surf} = \min(\alpha S_{ut}^{\beta}, 1) \quad (10.4)$$

Table 10.1:

Surface Finish	α if S_{ut} in kpsi	α if S_{ut} in MPa	β
Ground	1.34	1.58	-0.085
Machined or cold-drawn	2.70	4.51	-0.265
Hot-rolled	14.4	57.7	-0.718
As-forged	39.9	272	-0.995

10.2.2 Size

Larger structures have a higher volume and thus an increased probability of containing structural flaws. The test specimens upon which the unmodified endurance limit is estimated are small in size. This correction is needed to account for these size differences.

Mischke provides the following

10.3 Fully Reversed Load

10.4 Simple Fluctuating Load

10.5 Combined Fluctuating Loads

10.6 Complex Loads

Appendix A

Cylinder Theory Derivation

We will find the stress in a cylinder by using a free-body diagram approach (Fig. A.1). σ_r is called the radial stress, σ_θ is the tangential stress or hoop stress, and σ_z is the longitudinal or axial stress. There are no shear stresses in this coordinate system.

A force balance yields

$$(\sigma_r + d\sigma_r)(r + dr)d\theta dz - \sigma_r(r d\theta dz) = 2\sigma_\theta(dr dz) \sin(d\theta/2) \quad (\text{A.1})$$

Because we are looking at a differential element $\sin \theta \simeq \theta$, and after simplification yields

$$\sigma_r dr + d\sigma_r(r + dr) = \sigma_\theta dr \quad (\text{A.2})$$

The product of differentiables $dr d\sigma_r$ can be considered negligible compared to the other terms. This gives

$$\sigma_r dr + r d\sigma_r = \sigma_\theta dr \quad (\text{A.3})$$

which can be written as

$$(\sigma_\theta - \sigma_r) = r \frac{d\sigma_r}{dr} \quad (\text{A.4})$$

This same result can be found purely mathematically by starting with the compatibility equations for a linearly elastic structure (Eq. (A.5)), which is just a statement of static equilibrium.

$$\nabla \cdot \boldsymbol{\sigma} = 0 \quad (\text{A.5})$$

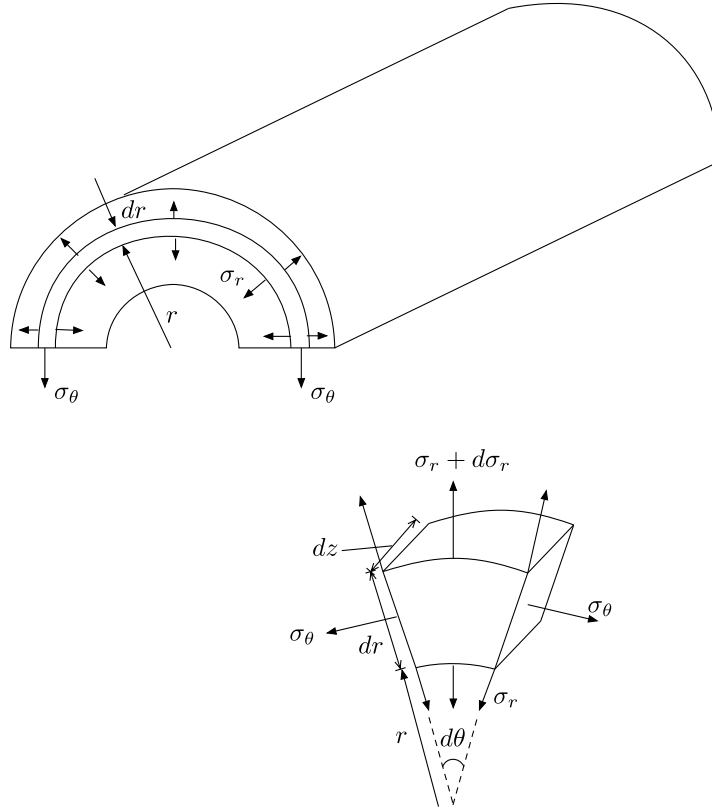


Figure A.1: Stress on a radial slice within the cylinder, and then on a small wedge within that slice.

We will expand this equation in cylindrical coordinates

$$\frac{\partial \sigma_r}{\partial r} + \frac{1}{r} \frac{\partial \tau_{r\theta}}{\partial \theta} + \frac{\partial \tau_{rz}}{\partial z} + \frac{1}{r} (\sigma_r - \sigma_\theta) = 0 \quad (\text{A.6})$$

$$\frac{1}{r^2} \frac{\partial (r^2 \tau_{r\theta})}{\partial r} + \frac{1}{r} \frac{\partial \sigma_\theta}{\partial \theta} + \frac{\partial \tau_{\theta z}}{\partial z} = 0 \quad (\text{A.7})$$

$$\frac{1}{r} \frac{\partial (r \tau_{rz})}{\partial r} + \frac{1}{r} \frac{\partial \tau_{\theta z}}{\partial \theta} + \frac{\partial \sigma_z}{\partial z} = 0 \quad (\text{A.8})$$

We assume symmetry such that deformations are independent of θ and assume we are far from an end so that deformations are independent of z (thus, all partial derivatives with respect to θ and z drop out). Then, the second and third equation result in

$$\tau_{r\theta} = \frac{C_1}{r^2} \quad (\text{A.9})$$

$$\tau_{rz} = \frac{C_2}{r} \quad (\text{A.10})$$

Since the shear stress is zero at the free surface, the constants C_1 and C_2 must be zero, and thus both of these shear stresses are zero throughout the cylinder. The first equation then simplifies to give the the same result as Eq. (A.4).

Just as we is done in deriving beam bending equations, we will assume that plane sections remain plane. This means that the longitudinal strain ϵ_z must be constant across the cross-section. We also assume that the longitudinal stress is constant (at least away from the walls). Then from the stress-strain relationships

$$\epsilon_z = \frac{1}{E} [\sigma_z - \nu(\sigma_r + \sigma_\theta)] \quad (\text{A.11})$$

we know that $\sigma_r + \sigma_\theta$ must also be a constant. Let us set that constant as $2A$

$$\sigma_r + \sigma_\theta = 2A \quad (\text{A.12})$$

If we sub σ_θ from Eq. (A.12) into Eq. (A.4) we have

$$(2A - 2\sigma_r) = r \frac{d\sigma_r}{dr} \quad (\text{A.13})$$

We now multiply through by r to get

$$2r\sigma_r + r^2 \frac{d\sigma_r}{dr} - 2Ar = 0 \quad (\text{A.14})$$

That was done so that we can pull out a differential

$$d(r^2\sigma_r - Ar^2) = 0 \quad (\text{A.15})$$

This implies that $r^2\sigma_r - Ar^2$ is a constant which we set to B . This gives

$$\sigma_r = A + \frac{B}{r^2} \quad (\text{A.16})$$

and substituting back into Eq. (A.12) we have

$$\sigma_\theta = A - \frac{B}{r^2} \quad (\text{A.17})$$

These equations are called the Lamé equations and are the basis for our equations on cylindrical stress. As we will see the longitudinal stress is also related

$$\sigma_z = A \quad (\text{A.18})$$

The boundary conditions of the problem will determine the unknown constants.

We can solve for the radial and tangential stress in a pressurized thick cylinder by applying the boundary conditions. At $\sigma_r(r_o) = -p_o$ and $\sigma_r(r_i) = -p_i$. In both cases, the sign is negative because the pressure causes compression. If we plug in our boundary conditions into Eq. (A.16) we get

$$\begin{aligned} A + \frac{B}{r_i^2} &= -p_i \\ A + \frac{B}{r_o^2} &= -p_o \end{aligned} \quad (\text{A.19})$$

This gives us two equations to solve for the unknown constants. The result is

$$\begin{aligned} A &= \frac{p_i r_i^2 - p_o r_o^2}{r_o^2 - r_i^2} \\ B &= \frac{(p_o - p_i) r_i^2 r_o^2}{r_o^2 - r_i^2} \end{aligned} \quad (\text{A.20})$$

We now have the radial and tangential stress in a pressurized cylinder

$$\sigma_r(r) = \frac{p_i r_i^2 - p_o r_o^2 + r_i^2 r_o^2 (p_o - p_i)/r^2}{r_o^2 - r_i^2} \quad (\text{A.21})$$

$$\sigma_\theta(r) = \frac{p_i r_i^2 - p_o r_o^2 - r_i^2 r_o^2 (p_o - p_i)/r^2}{r_o^2 - r_i^2} \quad (\text{A.22})$$

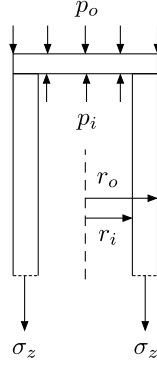


Figure A.2: Longitudinal stress balances by pressure acting on cylinder.

The longitudinal stress can be found from a simple force balance (see Fig. A.2):

$$\begin{aligned}
 p_i r_i^2 - p_o r_o^2 &= \sigma_z (r_o^2 - r_i^2) \\
 \Rightarrow \sigma_z &= \frac{p_i r_i^2 - p_o r_o^2}{r_o^2 - r_i^2} \\
 \sigma_z &= A
 \end{aligned} \tag{A.23}$$

Note that σ_z is halfway between σ_r and σ_θ .

Appendix B

Unsymmetric Bending Derivation

Unsymmetric bending occurs if a beam does not have a longitudinal plane of symmetry, or if the loads are not aligned with that plane of symmetry. For unsymmetric bending the cross section will rotate about a neutral axis that is not necessarily parallel to the moment. Even when there is not a plane of symmetry, experiments show that plane sections remain plane. This implies that ϵ_x (where x is the axial direction) must vary linearly with distance from the neutral axis. We also make the assumption that the other normal stresses are negligible compared to the axial stress. In other words we assume $\sigma_x = E\epsilon_x$. This means the stress is also a linear function, which we can write in a general form for some unknown constants:

$$\sigma_x = a + by + cz \quad (\text{B.1})$$

We choose a coordinate system coincident with the centroid of the cross section. For static equilibrium the stress resultants must balance the applied loads.

$$0 = \int \sigma_x dA \quad (\text{B.2})$$

$$M_y = \int z \sigma_x dA \quad (\text{B.3})$$

$$M_z = - \int y \sigma_x dA \quad (\text{B.4})$$

$$(\text{B.5})$$

Substituting in Eq. (B.1) into the first integral gives:

$$0 = aA + b \int y dA + c \int z dA \quad (\text{B.6})$$

The second and third term must be zero because we are integrating about the centroidal axis. This implies that:

$$\begin{aligned} 0 &= aA \\ \Rightarrow a &= 0 \end{aligned} \quad (\text{B.7})$$

Because $a = 0$ this means the neutral axis must pass through the centroid ($y = 0, z = 0$). The second integral gives

$$\begin{aligned} M_y &= b \int yz dA + c \int z^2 dA \\ M_y &= bI_{yz} + cI_y \end{aligned} \quad (\text{B.8})$$

Finally, the third equation results in

$$\begin{aligned} M_z &= -b \int y^2 dA - c \int yz dA \\ M_z &= -bI_z - cI_{yz} \end{aligned} \quad (\text{B.9})$$

Equations (B.8) and (B.9) yields two equations for two unknowns which we can solve as

$$\begin{aligned} b &= \frac{-M_y I_{yz} - M_z I_y}{I_y I_z - I_{yz}^2} \\ c &= \frac{M_y I_z + M_z I_{yz}}{I_y I_z - I_{yz}^2} \end{aligned} \quad (\text{B.10})$$

We now have a formula for the flexural stress for unsymmetric bending

$$\sigma_x = \frac{(-M_y I_{yz} - M_z I_y)y + (M_y I_z + M_z I_{yz})z}{I_y I_z - I_{yz}^2} \quad (\text{B.11})$$

The neutral axis is found by setting $\sigma_x = 0$ and noting that the angle of the neutral axis, λ , must follow from $\tan \lambda = z/y$. The result is

$$\tan \lambda = \frac{M_y I_{yz} + M_z I_y}{M_y I_z + M_z I_{yz}} \quad (\text{B.12})$$

The coordinate system y, z can be of any orientation, but must pass through the centroid. If y and z are also principal axes then $I_{yz} = 0$ and the flexural stress formula reduces to the basic biaxial bending equation

$$\sigma_x = -\frac{M_z y}{I_z} + \frac{M_y z}{I_y} \quad (\text{B.13})$$

Appendix C

Standard Normal Table

The following pages tabulate the cumulative distribution function (CDF) for a normal distribution as a function of normalized input z :

$$z = \frac{x - \mu}{\sigma} \tag{C.1}$$

The CDF is visualized in Fig. C.1.

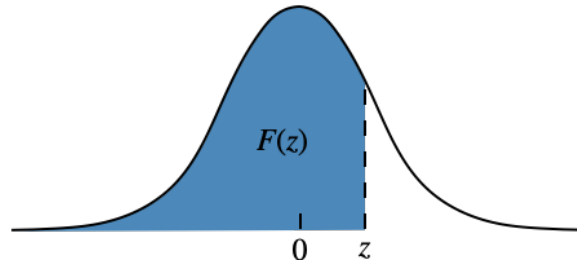


Figure C.1: A visualization of the cumulative distribution function.

z	$F(z)$	z	$F(z)$	z	$F(z)$	z	$F(z)$
0.00	0.500000	0.38	0.648027	0.76	0.776373	1.14	0.872857
0.01	0.503989	0.39	0.651732	0.77	0.779350	1.15	0.874928
0.02	0.507978	0.40	0.655422	0.78	0.782305	1.16	0.876976
0.03	0.511966	0.41	0.659097	0.79	0.785236	1.17	0.879000
0.04	0.515953	0.42	0.662757	0.80	0.788145	1.18	0.881000
0.05	0.519939	0.43	0.666402	0.81	0.791030	1.19	0.882977
0.06	0.523922	0.44	0.670031	0.82	0.793892	1.20	0.884930
0.07	0.527903	0.45	0.673645	0.83	0.796731	1.21	0.886861
0.08	0.531881	0.46	0.677242	0.84	0.799546	1.22	0.888768
0.09	0.535856	0.47	0.680822	0.85	0.802337	1.23	0.890651
0.10	0.539828	0.48	0.684386	0.86	0.805105	1.24	0.892512
0.11	0.543795	0.49	0.687933	0.87	0.807850	1.25	0.894350
0.12	0.547758	0.50	0.691462	0.88	0.810570	1.26	0.896165
0.13	0.551717	0.51	0.694974	0.89	0.813267	1.27	0.897958
0.14	0.555670	0.52	0.698468	0.90	0.815940	1.28	0.899727
0.15	0.559618	0.53	0.701944	0.91	0.818589	1.29	0.901475
0.16	0.563559	0.54	0.705401	0.92	0.821214	1.30	0.903200
0.17	0.567495	0.55	0.708840	0.93	0.823814	1.31	0.904902
0.18	0.571424	0.56	0.712260	0.94	0.826391	1.32	0.906582
0.19	0.575345	0.57	0.715661	0.95	0.828944	1.33	0.908241
0.20	0.579260	0.58	0.719043	0.96	0.831472	1.34	0.909877
0.21	0.583166	0.59	0.722405	0.97	0.833977	1.35	0.911492
0.22	0.587064	0.60	0.725747	0.98	0.836457	1.36	0.913085
0.23	0.590954	0.61	0.729069	0.99	0.838913	1.37	0.914657
0.24	0.594835	0.62	0.732371	1.00	0.841345	1.38	0.916207
0.25	0.598706	0.63	0.735653	1.01	0.843752	1.39	0.917736
0.26	0.602568	0.64	0.738914	1.02	0.846136	1.40	0.919243
0.27	0.606420	0.65	0.742154	1.03	0.848495	1.41	0.920730
0.28	0.610261	0.66	0.745373	1.04	0.850830	1.42	0.922196
0.29	0.614092	0.67	0.748571	1.05	0.853141	1.43	0.923641
0.30	0.617911	0.68	0.751748	1.06	0.855428	1.44	0.925066
0.31	0.621720	0.69	0.754903	1.07	0.857690	1.45	0.926471
0.32	0.625516	0.70	0.758036	1.08	0.859929	1.46	0.927855
0.33	0.629300	0.71	0.761148	1.09	0.862143	1.47	0.929219
0.34	0.633072	0.72	0.764238	1.10	0.864334	1.48	0.930563
0.35	0.636831	0.73	0.767305	1.11	0.866500	1.49	0.931888
0.36	0.640576	0.74	0.770350	1.12	0.868643	1.50	0.933193
0.37	0.644309	0.75	0.773373	1.13	0.870762	1.51	0.934478

z	$F(z)$	z	$F(z)$	z	$F(z)$	z	$F(z)$
1.52	0.935745	1.90	0.971283	2.28	0.988696	2.66	0.996093
1.53	0.936992	1.91	0.971933	2.29	0.988989	2.67	0.996207
1.54	0.938220	1.92	0.972571	2.30	0.989276	2.68	0.996319
1.55	0.939429	1.93	0.973197	2.31	0.989556	2.69	0.996427
1.56	0.940620	1.94	0.973810	2.32	0.989830	2.70	0.996533
1.57	0.941792	1.95	0.974412	2.33	0.990097	2.71	0.996636
1.58	0.942947	1.96	0.975002	2.34	0.990358	2.72	0.996736
1.59	0.944083	1.97	0.975581	2.35	0.990613	2.73	0.996833
1.60	0.945201	1.98	0.976148	2.36	0.990863	2.74	0.996928
1.61	0.946301	1.99	0.976705	2.37	0.991106	2.75	0.997020
1.62	0.947384	2.00	0.977250	2.38	0.991344	2.76	0.997110
1.63	0.948449	2.01	0.977784	2.39	0.991576	2.77	0.997197
1.64	0.949497	2.02	0.978308	2.40	0.991802	2.78	0.997282
1.65	0.950529	2.03	0.978822	2.41	0.992024	2.79	0.997365
1.66	0.951543	2.04	0.979325	2.42	0.992240	2.80	0.997445
1.67	0.952540	2.05	0.979818	2.43	0.992451	2.81	0.997523
1.68	0.953521	2.06	0.980301	2.44	0.992656	2.82	0.997599
1.69	0.954486	2.07	0.980774	2.45	0.992857	2.83	0.997673
1.70	0.955435	2.08	0.981237	2.46	0.993053	2.84	0.997744
1.71	0.956367	2.09	0.981691	2.47	0.993244	2.85	0.997814
1.72	0.957284	2.10	0.982136	2.48	0.993431	2.86	0.997882
1.73	0.958185	2.11	0.982571	2.49	0.993613	2.87	0.997948
1.74	0.959070	2.12	0.982997	2.50	0.993790	2.88	0.998012
1.75	0.959941	2.13	0.983414	2.51	0.993963	2.89	0.998074
1.76	0.960796	2.14	0.983823	2.52	0.994132	2.90	0.998134
1.77	0.961636	2.15	0.984222	2.53	0.994297	2.91	0.998193
1.78	0.962462	2.16	0.984614	2.54	0.994457	2.92	0.998250
1.79	0.963273	2.17	0.984997	2.55	0.994614	2.93	0.998305
1.80	0.964070	2.18	0.985371	2.56	0.994766	2.94	0.998359
1.81	0.964852	2.19	0.985738	2.57	0.994915	2.95	0.998411
1.82	0.965620	2.20	0.986097	2.58	0.995060	2.96	0.998462
1.83	0.966375	2.21	0.986447	2.59	0.995201	2.97	0.998511
1.84	0.967116	2.22	0.986791	2.60	0.995339	2.98	0.998559
1.85	0.967843	2.23	0.987126	2.61	0.995473	2.99	0.998605
1.86	0.968557	2.24	0.987455	2.62	0.995604	3.00	0.998650
1.87	0.969258	2.25	0.987776	2.63	0.995731	3.01	0.998694
1.88	0.969946	2.26	0.988089	2.64	0.995855	3.02	0.998736
1.89	0.970621	2.27	0.988396	2.65	0.995975	3.03	0.998777

z	$F(z)$	z	$F(z)$	z	$F(z)$	z	$F(z)$
3.04	0.998817	3.42	0.999687	3.80	0.999928	4.18	0.999985
3.05	0.998856	3.43	0.999698	3.81	0.999931	4.19	0.999986
3.06	0.998893	3.44	0.999709	3.82	0.999933	4.20	0.999987
3.07	0.998930	3.45	0.999720	3.83	0.999936	4.21	0.999987
3.08	0.998965	3.46	0.999730	3.84	0.999938	4.22	0.999988
3.09	0.998999	3.47	0.999740	3.85	0.999941	4.23	0.999988
3.10	0.999032	3.48	0.999749	3.86	0.999943	4.24	0.999989
3.11	0.999065	3.49	0.999758	3.87	0.999946	4.25	0.999989
3.12	0.999096	3.50	0.999767	3.88	0.999948	4.26	0.999990
3.13	0.999126	3.51	0.999776	3.89	0.999950	4.27	0.999990
3.14	0.999155	3.52	0.999784	3.90	0.999952	4.28	0.999991
3.15	0.999184	3.53	0.999792	3.91	0.999954	4.29	0.999991
3.16	0.999211	3.54	0.999800	3.92	0.999956	4.30	0.999991
3.17	0.999238	3.55	0.999807	3.93	0.999958	4.31	0.999992
3.18	0.999264	3.56	0.999815	3.94	0.999959	4.32	0.999992
3.19	0.999289	3.57	0.999822	3.95	0.999961	4.33	0.999993
3.20	0.999313	3.58	0.999828	3.96	0.999963	4.34	0.999993
3.21	0.999336	3.59	0.999835	3.97	0.999964	4.35	0.999993
3.22	0.999359	3.60	0.999841	3.98	0.999966	4.36	0.999993
3.23	0.999381	3.61	0.999847	3.99	0.999967	4.37	0.999994
3.24	0.999402	3.62	0.999853	4.00	0.999968	4.38	0.999994
3.25	0.999423	3.63	0.999858	4.01	0.999970	4.39	0.999994
3.26	0.999443	3.64	0.999864	4.02	0.999971	4.40	0.999995
3.27	0.999462	3.65	0.999869	4.03	0.999972	4.41	0.999995
3.28	0.999481	3.66	0.999874	4.04	0.999973	4.42	0.999995
3.29	0.999499	3.67	0.999879	4.05	0.999974	4.43	0.999995
3.30	0.999517	3.68	0.999883	4.06	0.999975	4.44	0.999996
3.31	0.999534	3.69	0.999888	4.07	0.999976	4.45	0.999996
3.32	0.999550	3.70	0.999892	4.08	0.999977	4.46	0.999996
3.33	0.999566	3.71	0.999896	4.09	0.999978	4.47	0.999996
3.34	0.999581	3.72	0.999900	4.10	0.999979	4.48	0.999996
3.35	0.999596	3.73	0.999904	4.11	0.999980	4.49	0.999996
3.36	0.999610	3.74	0.999908	4.12	0.999981	4.50	0.999997
3.37	0.999624	3.75	0.999912	4.13	0.999982	4.51	0.999997
3.38	0.999638	3.76	0.999915	4.14	0.999983	4.52	0.999997
3.39	0.999651	3.77	0.999918	4.15	0.999983	4.53	0.999997
3.40	0.999663	3.78	0.999922	4.16	0.999984	4.54	0.999997
3.41	0.999675	3.79	0.999925	4.17	0.999985	4.55	0.999997